

# Creation of Dirac neutrinos in a dense medium with a time-dependent effective potential

Maxim Dvornikov<sup>a,b,c,\*</sup>, S. P. Gavrilov<sup>a,d,†</sup> and D. M. Gitman<sup>a,e,‡</sup>

<sup>a</sup>*Institute of Physics, University of São Paulo, CP 66318,  
CEP 05315-970 São Paulo, SP, Brazil;*

<sup>b</sup>*Research School of Physics and Engineering,  
Australian National University,  
Canberra ACT 2601, Australia;*

<sup>c</sup>*Pushkov Institute of Terrestrial Magnetism,  
Ionosphere and Radiowave Propagation (IZMIRAN),  
142190 Troitsk, Moscow, Russia;*

<sup>d</sup>*Department of General and Experimental Physics,  
Herzen State Pedagogical University of Russia,  
Moyka embankment 48, 191186 St. Petersburg, Russia*

<sup>e</sup>*Department of Physics,  
Tomsk State University, 634050, Tomsk, Russia*

(Dated: February 27, 2022)

We consider Dirac neutrinos interacting with background fermions in the frame of the standard model. We demonstrate that a time-dependent effective potential is quite possible in a protoneutron star (PNS) at certain stages of its evolution. For the first time, we formulate a nonperturbative treatment of neutrino processes in a matter with arbitrary time-dependent effective potential. Using linearly growing effective potential, we study the typical case of a slowly varying matter interaction potential. We calculate differential mean numbers of  $\nu\bar{\nu}$  pairs created from the vacuum by this potential and find that they crucially depend on the magnitude of masses of the lightest neutrino eigenstate. These distributions uniformly span up to  $\sim 10$  eV energies for muon and tau neutrinos created in PNS core due to the compression just before the hydrodynamic bounce and up to  $\sim 0.1$  eV energies for all three active neutrino flavors created in the neutronization. Considering different stages of the PNS evolution, we derive constraints on neutrino masses,  $m_\nu \lesssim (10^{-8} - 10^{-7})$  eV, corresponding to the nonvanishing  $\nu\bar{\nu}$  pairs flux produced by this mechanism. We show that one can distinguish such coherent flux from chaotic fluxes of any other origin. Part of these neutrinos, depending on the flavor and helicity, are bounded in the PNS, while antineutrinos of any flavor escape the PNS. If the created pairs are  $\nu_e\bar{\nu}_e$ , then a part of the corresponding neutrinos also escape the PNS. The detection of  $\nu$  and  $\bar{\nu}$  with such low energies is beyond current experimental techniques.

PACS numbers: 13.15.+g, 97.60.Bw, 95.85.Ry, 14.60.Pq

Keywords: nonperturbative vacuum pair production, massive Dirac neutrino, background matter, supernova

## I. INTRODUCTION

Particle creation from the vacuum by strong electromagnetic, Yang Mills, and gravitational fields is a well-known nonlinear quantum phenomenon which has many applications in modern high-energy physics. Its theoretical study has a long story that is described in numerous works, see for example Refs. [1–4]. Creation of charged particles from the vacuum by strong electric-like fields needs superstrong field magnitudes compared with Schwinger critical field  $E_{\text{cr}} = m^2 c^3 / e \hbar \simeq 1.3 \times 10^{16} \text{ V} \cdot \text{cm}^{-1}$  [5]. Nevertheless, recent progress in laser physics allows one to hope that this effect will be experimentally observed in the near future even in laboratory conditions,

see Ref. [6] for the review.<sup>1</sup> The particle creation from the vacuum by external electric and gravitational backgrounds plays also an important role in cosmology and astrophysics [2].

It should be noted that not only electric and gravitational macroscopic backgrounds may destabilize a quantum field vacuum. As it was shown in Ref. [8], the vacuum of neutrinos, possessing anomalous magnetic moments, becomes unstable in a strong inhomogeneous magnetic field such that the creation of neutrinos by the latter field may take place. Estimates presented in Ref. [8] show that this effect can be produced by strong magnetic fields of magnetars and fields generated during a supernova explosion and has to be taken into account in the astrophysics.

The instability of the neutrino vacuum exists also due to the neutrino interaction with a background matter.

\* maxim.dvornikov@anu.edu.au

† gavrilovsergeyp@yahoo.com

‡ gitman@if.usp.br

<sup>1</sup> Electron-hole pair creation from the vacuum was recently observed in graphene, see, for example, Ref. [7].

It should be noted that the neutrino-antineutrino ( $\nu\bar{\nu}$ ) pairs creation in a dense matter of a neutron star was studied in Refs. [9–13]. In Refs. [9–11] the matter density was supposed to be time-independent and the  $\nu\bar{\nu}$  pair creation was considered empirically by using the analogy between a neutron star potential and a potential well. In this case the production rate of the  $\nu\bar{\nu}$  pair creation was evaluated semiclassically borrowing the Schwinger’s result in QED for the probability for a vacuum to remain a vacuum [5]. The case of a time-dependent density was studied nonperturbatively, using numerical calculations, for an oscillating density of a neutron star, a supernova, and gamma ray bursts in Ref. [12] and perturbatively in Ref. [13]. It should be noted that the perturbation theory is valid only for nonrealistic high frequency density variations. Realistic  $\nu\bar{\nu}$  pairs creation due to a slowly varying matter interaction potential was not considered before.

In the present article we formulate a consistent non-perturbative approach for calculating, in the framework of QFT, the  $\nu\bar{\nu}$  pair production from the vacuum due to a coherent neutrino interaction with a background matter, in particular, a matter with arbitrary time-dependent effective potential. We apply then this approach to calculate the effect in some interesting cases of the medium evolution and distribution.

The article is organized as follows. In the beginning we describe a field theory model, which is used by us to treat neutrinos interacting with a background matter. Then, in the framework of the quantum version of the model, we consider a case of a matter with time-dependent effective potential. We show that such a background is quite possible at certain stages of a protoneutron star (PNS) evolution. For instance, one can discuss the matter compression in the PNS core just before the hydrodynamic bounce or the phase transition of a dense medium of PNS at the neutronization stage. Then, using a nonperturbative approach that is similar to the one developed in QED with time-dependent external electromagnetic fields, see Ref. [3], we formulate a calculation scheme for the neutrino production in the case under consideration. This technique is based on using complete sets of exact solutions of a modified Dirac equation for neutrinos interacting with a matter density. These solutions are used to quantize the neutrino field and introduce the corresponding in- and out- creation and annihilation operators. We represent the mean numbers of  $\nu\bar{\nu}$  pairs created and probabilities of all the transitions via coefficients of the corresponding Bogolyubov transformations. In particular, we derive general formulas that describe the  $\nu\bar{\nu}$  pair creation in the matter with linearly growing in time effective potential and study the typical case of a slowly varying matter interaction potential.

As a main application of the developed approach, we consider the  $\nu\bar{\nu}$  pair creation of Dirac neutrinos from the vacuum due to the compression in the core of PNS before the bounce and at the neutronization stage. We show that the behavior of the effective number density

at these stages of the PNS evolution can be described by a slowly varying in time homogeneous effective potential. Then we demonstrate that the intensity of the neutrino creation crucially depends on the magnitude of masses of the lightest neutrino eigenstate. We also find that the momentum distribution of  $\nu\bar{\nu}$  pairs is isotropic and uniform in the low-energy range (up to  $\sim 10$  eV) dropping sharply for higher energies. We find that if the mass of the lightest neutrino is small enough, the flux of pairs of the lightest  $\nu$  and  $\bar{\nu}$ , created from the vacuum during the stages of PNS evolution, may exceed the low-energy flux of any other origin. We derive constraints on neutrino masses corresponding to the nonvanishing  $\nu\bar{\nu}$  pairs flux produced from the vacuum due to the compression in the PNS before the bounce and at the neutronization stage. Finally, we list all the obtained results. Possible accompanying processes that might affect identification of this vacuum instability at the initial stages of the PNS evolution are examined in Appendix A. Some mathematical details are separated in Appendix B.

## II. INTERACTION OF DIRAC NEUTRINOS WITH BACKGROUND MATTER

Here we briefly consider the classical field theory description of massive Dirac neutrinos interacting with background fermionic matter.

The results of the recent experiments (see, e.g., Ref. [14]) explicitly demonstrate that neutrinos are massive particles and there is a nonzero mixing between different mass eigenstates. However, in some cases one can neglect the mixing in the neutrino sector. For example, it is the case when the corresponding transition probability of neutrino oscillations is suppressed. In such cases we can consider a single neutrino eigenstate having an effective mass  $m$ . It should be noted that the question whether neutrinos are Dirac or Majorana particles still remains open (see, e.g., Ref. [15]). In our constructions and further calculations we work with Dirac neutrinos. We suppose that the gravitational interaction of neutrinos is negligible and the effect of possible matter rotation is small for quantum processes under consideration.

The Lagrangian of a massive Dirac neutrino field  $\psi(X)$  interacting with a matter by an effective potential  $g_\mu(X)$  has the following form in the forward scattering approximation<sup>2</sup>

$$\mathcal{L} = \bar{\psi}(X) (i\gamma^\mu \partial_\mu - m) \psi(X) - g_\mu(X) \bar{\psi}(X) \gamma^\mu P_L \psi(X), \quad (2.1)$$

see Ref. [16]. Here  $\psi(X)$  is a Dirac spinor,  $X = (x^0 = t, \mathbf{r} = (x, y, z))$ ,  $\gamma^\mu = (\gamma^0, \boldsymbol{\gamma})$  are Dirac matrices,  $\gamma^5 = i\gamma^0\gamma^1\gamma^2\gamma^3$ , and  $P_L = (1 - \gamma^5)/2$  is the projector to

---

<sup>2</sup> Here we use the natural units in which  $\hbar = c = 1$ .

the left chiral states. In what follows, we use the Dirac matrices in the standard representation,

$$\gamma^0 = \begin{pmatrix} 1 & 0 \\ 0 & -1 \end{pmatrix}, \quad \gamma = \begin{pmatrix} 0 & \boldsymbol{\sigma} \\ -\boldsymbol{\sigma} & 0 \end{pmatrix},$$

$$\gamma^5 = \begin{pmatrix} 0 & 1 \\ 1 & 0 \end{pmatrix}, \quad (2.2)$$

where  $\boldsymbol{\sigma}$  are the Pauli matrices.

The effective potential  $g^\mu(X)$  that describes the matter interaction with neutrinos is a linear combination of the hydrodynamic currents  $j_f^\mu$  and polarizations  $\lambda_f^\mu$  of background fermions  $f$ ,

$$g^\mu(X) = \sqrt{2}G_F \sum_f \left( q_f^{(1)} j_f^\mu + q_f^{(2)} \lambda_f^\mu \right), \quad (2.3)$$

where  $G_F$  is the Fermi constant and coefficients  $q_f^{(1)}$  and  $q_f^{(2)}$  depend on the types of a neutrino and background fermions [17]. If we deal with electron neutrinos  $\nu_e$  propagating in the matter that is composed of electrons, protons, and neutrons, these coefficients have the form,

$$q_f^{(1)} = I_{L3}^{(f)} - 2Q_f \sin^2 \theta_W + \delta_{ef},$$

$$q_f^{(2)} = -I_{L3}^{(f)} - \delta_{ef}, \quad (2.4)$$

where  $I_{L3}^{(f)}$  is the third component of the weak isospin of the type  $f$  fermions,  $Q_f$  is their electric charge,  $\theta_W$  is the Weinberg angle, and  $\delta_{ef} = 1$  for electrons and vanishes for protons and neutrons. To get the coefficients  $q_f^{(1,2)}$  for muon and tau neutrinos  $\nu_{\mu,\tau}$  we should set  $\delta_{ef}$  to be zero in Eq. (2.4).

Let us consider first an electroneutral matter which is unpolarized and nonmoving. In this case the only zeroth component  $g(X) \equiv g^0(X)$  of  $g^\mu(X)$  is nonzero. Using Eq. (2.4), this component can be found in the following form,

$$g(X) = \sqrt{2}G_F n_{\text{eff}},$$

$$n_{\text{eff}} = \begin{cases} n_e - \frac{1}{2}n_n, & \text{for } \nu_e, \\ -\frac{1}{2}n_n, & \text{for } \nu_{\mu,\tau}, \end{cases} \quad (2.5)$$

where  $n_e$  and  $n_n$  are the electron and neutron densities respectively. The difference in the effective potentials for  $\nu_e$  and  $\nu_{\mu,\tau}$  in Eq. (2.5) is owing to the fact that, besides neutral current interactions,  $\nu_e$  is also involved in the charged current interactions with the given matter.

The Lagrangian (2.1) implies the following equations of motion,

$$(i\gamma^\mu \partial_\mu - m - g(X) \gamma^0 P_L) \psi(X) = 0. \quad (2.6)$$

In general case the effective potential depends on all the space-time coordinates  $X$ . In the following we shall restrict ourselves to the case when  $g(X)$  is homogeneous and depends only on the time  $t$ .

This model can be applied for the description of neutrinos in realistic conditions like a dense matter of PNS. Note that the matter of PNS with the high degree of accuracy can be taken as spatially homogeneous [18]. At certain stages of the supernova explosion the effective potential can be regarded as a function of time only. For example, just before the hydrodynamic bounce the matter density in PNS core increases several orders of magnitude. Another situation when the effective potential can be time dependent happens outside the core at the neutronization stage. Indeed, a typical PNS has  $n_n \approx n_e \approx n_p$  before the neutronization. We can take that  $n_e = n_p \approx 0$  in some regions outside the PNS core after the neutronization. Therefore, using Eq. (2.5), we get that the value  $g$  varies from the initial  $g(t_{\text{in}})$  to the final  $g(t_{\text{out}})$  as

$$g(t_{\text{out}}) = \begin{cases} -2g(t_{\text{in}}) & \text{for } \nu_e \\ +2g(t_{\text{in}}) & \text{for } \nu_{\mu,\tau} \end{cases}. \quad (2.7)$$

Thus the time-dependent effective potential is quite possible in PNS. As is demonstrated below, it is the time dependence of  $g$  which stipulates the instability of the neutrino vacuum and results in a coherent  $\nu\bar{\nu}$  pairs creation.

One can see that the inhomogeneity of PNS matter near the star surface affects the neutrino motion in the PNS crust and somehow influences the neutrino creation. This effect requires a separate consideration. We shall briefly discuss it in Appendix A.

Since  $g$  is uniform, we can choose the Dirac spinor in the following form:

$$\psi(X) = \exp \left[ -\frac{i}{2} \int_{t_0}^t g(t') dt' \right] \tilde{\psi}(X), \quad (2.8)$$

where the spinor  $\tilde{\psi}(X)$  satisfies the equation

$$i\partial_0 \tilde{\psi}(X) = H(t) \tilde{\psi}(X),$$

$$H(t) = \gamma^0 (-i\nabla \gamma + m) - \frac{1}{2} g(t) \gamma^5. \quad (2.9)$$

One can see that the time-dependent Hamiltonian  $H(t)$  is the kinetic energy operator. Note that the Dirac Hamiltonian that corresponds to the untransformed Eq. (2.6) is  $H(t) + g(t)/2$ . However, the Hamiltonian  $H(t)$  plays an important role in the physical interpretation of states vectors. It should be also noted that in our case when  $\nabla g = 0$ , both the momentum operator  $-i\nabla$  and the helicity operator,

$$\Xi = \frac{-i\nabla \Sigma}{\sqrt{(-i\nabla)^2}}, \quad \Sigma = \gamma^5 \gamma^0 \gamma = \begin{pmatrix} \boldsymbol{\sigma} & 0 \\ 0 & \boldsymbol{\sigma} \end{pmatrix}, \quad (2.10)$$

commute with  $H(t)$ .

Using Eq. (2.8) we can verify that the inner product of arbitrary solutions  $\psi$  and  $\psi'$  is reduced to the inner product of the corresponding solutions  $\tilde{\psi}$  and  $\tilde{\psi}'$ ,

$$(\psi, \psi') = \int \psi^\dagger(t, \mathbf{r}) \psi'(t, \mathbf{r}) d\mathbf{r} = (\tilde{\psi}, \tilde{\psi}'), \quad (2.11)$$

and is conserved.

In what follows, we assume that  $m \neq 0$ . In this case  $\gamma^5$  does not commute with the Hamiltonian  $H(t)$ . Then, using the representation

$$\tilde{\psi}(X) = [i\partial_0 + H(t)]\phi(X), \quad (2.12)$$

we obtain the second-order differential equation for the spinor  $\phi(X)$ ,

$$\left\{ (\partial_0)^2 + [H(t)]^2 + \frac{i}{2}\gamma^5\partial_0 g(t) \right\} \phi(X) = 0. \quad (2.13)$$

In particular, this equation describes the influence of the time dependence of  $g(t)$  on neutrino wave functions.

If  $m = 0$ , the matrix  $\gamma^5$  commutes with  $H(t)$  and Eq. (2.6) can be separated into two independent equations,

$$\begin{aligned} i\partial_0\psi_{L,R}(X) &= \left[ H_0(t) + \frac{1}{2}(1 \pm 1)g(t) \right] \psi_{L,R}(X), \\ H_0(t) &= \gamma^0(-i\nabla\gamma + m), \end{aligned} \quad (2.14)$$

for the spinors  $\psi_{L,R}(X) = \frac{1}{2}(1 \mp \gamma^5)\psi(X)$ . Equation (2.14) is a first-order differential equation with respect of time. The spinors  $\psi_R(X)$  and

$$\exp\left[+i\int_{t_0}^t g(t')dt'\right]\psi_L(X), \quad (2.15)$$

describe free neutrinos and antineutrinos since the potential  $g(t)$  is absent in equations for these quantities. Of course, it is a consequence of our supposition that  $g(X)$  is uniform. If, however,  $\nabla g(X) \neq 0$ , the left neutrinos are not free anymore. Hence the scale of the possible matter inhomogeneity  $L$  has to be big enough, e.g.,  $L \gg 1/m$ .

### III. QUANTIZATION IN TERMS OF ADEQUATE PARTICLES AND ANTIPARTICLES

In this section we use results of the canonical quantization of the Lagrangian in Eq. (2.1) described in Ref. [19]. We start with the constant and uniform effective potential. Then we consider the matter with time-dependent effective potential. Using the corresponding exact solutions of the Dirac equation, we introduce creation and annihilation operators which diagonalize the kinetic energy operator. The latter operator has a positive spectrum either in the initial or in the final time instants. We construct the initial and final Fock spaces and physical quantities that will be calculated in what follows.

#### A. Constant effective potential

We start with the case when  $g = \text{const} \neq 0$ . Here the one-particle description is possible, such that one can speak about one neutrino moving in a homogeneous

matter with a constant effective potential. Then the Hamiltonian  $H(t) = H$  is time independent. The corresponding solutions of the Dirac equation are plane waves  $\psi(X) \sim \exp(-ip_\mu X^\mu)$ . Particles in such states have the following kinetic energies  $\mathcal{E}$  [20],

$$\mathcal{E} = \sqrt{m^2 + \left(p - \sigma \frac{g}{2}\right)^2}, \quad (3.1)$$

where  $p = |\mathbf{p}|$ ,  $\mathbf{p}$  is the neutrino momentum, and  $\sigma = \pm 1$  is the eigenvalue of the neutrino helicity operator given by Eq. (2.10). The total energies  $p_0^{(\pm)}$  differ from the kinetic energies by a constant value,  $p_0^{(\pm)} = \pm\mathcal{E} + g/2$ , since the density  $g$  is homogeneous.

We represent wave functions under consideration as follows,

$$\begin{aligned} +\psi(t, \mathbf{r}) &\sim u_\sigma(\mathbf{p}) \exp\left[-ip_0^{(+)}t + i\mathbf{p}\mathbf{r}\right], \\ -\psi(t, \mathbf{r}) &\sim v_\sigma(\mathbf{p}) \exp\left[-ip_0^{(-)}t + i\mathbf{p}\mathbf{r}\right], \end{aligned} \quad (3.2)$$

where the basis spinors  $u_\sigma(\mathbf{p})$  and  $v_\sigma(\mathbf{p})$  have the form

$$\begin{aligned} u_\sigma &= \sqrt{\frac{m + \mathcal{E}}{2\mathcal{E}}} \begin{pmatrix} w_\sigma \\ \frac{\sigma p - g/2}{m + \mathcal{E}} w_\sigma \end{pmatrix}, \\ v_\sigma &= \sqrt{\frac{m + \mathcal{E}}{2\mathcal{E}}} \begin{pmatrix} -\frac{\sigma p - g/2}{m + \mathcal{E}} w_\sigma \\ w_\sigma \end{pmatrix}, \end{aligned} \quad (3.3)$$

and  $w_\sigma = w_\sigma(\mathbf{p})$  are the two-component helicity amplitudes (see Ref. [21]). These spinors satisfy the following orthonormality conditions and completeness relations:

$$\begin{aligned} u_\sigma^\dagger(\mathbf{p})u_{\sigma'}(\mathbf{p}) &= \delta_{\sigma\sigma'}, \quad v_\sigma^\dagger(\mathbf{p})v_{\sigma'}(\mathbf{p}) = \delta_{\sigma\sigma'}, \\ u_\sigma^\dagger(\mathbf{p})v_{\sigma'}(\mathbf{p}) &= 0, \\ \sum_\sigma [u_\sigma(\mathbf{p}) \otimes u_\sigma^\dagger(\mathbf{p}) + v_\sigma(\mathbf{p}) \otimes v_\sigma^\dagger(\mathbf{p})] &= 1. \end{aligned} \quad (3.4)$$

It is important to note that in the framework of the quantum field theory, taking into account the fermion nature of neutrinos, one can see that  $+\psi(t, \mathbf{r})$  describes neutrino states with the kinetic energy  $p_0^{(+)} - g/2 = \mathcal{E}$ , while  $-\psi(t, \mathbf{r})$  describes antineutrino states with the kinetic energy  $|p_0^{(-)} - g/2| = \mathcal{E}$ . One can also see that the corresponding neutrinos and antineutrinos behave like free particles.

#### B. Time-dependent effective potential

In the case of a time-dependent effective potential  $g(t)$ , the Hamiltonian  $H(t)$  is also time dependent, and  $H(t)$  and  $H(t')$  do not commute if  $t \neq t'$ . Using our experience in QED with external time-dependent backgrounds, we believe that the one-particle description is not applicable in such a case. To consider nonperturbative effects, we have to use the approach developed in QED and known as the generalized Furry representation (see

Refs. [3, 4]). Below, we show that the problem in question can be treated in the similar manner.

After the quantization,  $\psi(X) = \psi(t, \mathbf{r})$  turns out to be the Heisenberg operator  $\Psi(X) = \Psi(t, \mathbf{r})$ . This operator obeys both the Dirac equation [Eq. (2.9)] and the standard equal time anticommutation relations:

$$\begin{aligned} [\Psi(t, \mathbf{r}), \Psi(t, \mathbf{r}') ]_+ &= [\Psi^\dagger(t, \mathbf{r}), \Psi^\dagger(t, \mathbf{r}') ]_+ = 0, \\ [\Psi(t, \mathbf{r}), \Psi^\dagger(t, \mathbf{r}') ]_+ &= \delta(\mathbf{r} - \mathbf{r}'). \end{aligned} \quad (3.5)$$

The second quantized Hamiltonian  $\hat{H}$  and the corresponding momentum and helicity operators have the following forms:

$$\hat{H}(t) = \int \Psi^\dagger(t, \mathbf{r}) H(t) \Psi(t, \mathbf{r}) d\mathbf{r} + H_0(t), \quad (3.6)$$

$$\begin{aligned} \hat{\mathbf{p}} &= \frac{1}{2} \int [\Psi^\dagger(t, \mathbf{r}), (-i\nabla) \Psi(t, \mathbf{r}) ]_- d\mathbf{r}, \\ \hat{\Xi} &= \frac{1}{2} \int [\Psi^\dagger(t, \mathbf{r}), \Xi \Psi(t, \mathbf{r}) ]_- d\mathbf{r}, \end{aligned} \quad (3.7)$$

where the  $c$  number (generally infinite) term  $H_0(t)$  corresponds to the energy of vacuum fluctuations. A definition of the corresponding vacuum is discussed just below.

Let us suppose that the effective potential  $g(t)$  is constant for  $t < t_1$  and for  $t > t_2$ . Therefore initial (at  $t < t_1$ ) and final (at  $t > t_2$ ) vacua are vacuum states of in- and out- particles which correspond to the constant effective potentials  $g(t_1) = g_1$  and  $g(t_2) = g_2$ , respectively. During the time interval  $t_2 - t_1 = T$ , the neutrino field interacts with the time-dependent effective potential  $g(t)$ . The initial and final vacua do not coincide because of the difference in the initial and final constant values  $g_1$  and  $g_2$ . Then we construct independently both initial and final Fock spaces in the Heisenberg representation. We introduce an initial set of creation and annihilation operators  $a_n^\dagger(\text{in})$ ,  $a_n(\text{in})$  of in-particles (neutrinos), and operators  $b_n^\dagger(\text{in})$ ,  $b_n(\text{in})$  of in-antiparticles (antineutrinos), the corresponding in-vacuum being  $|0, \text{in}\rangle$ , and a final set of creation and annihilation operators  $a_n^\dagger(\text{out})$ ,  $a_n(\text{out})$  of out-neutrinos and operators  $b_n^\dagger(\text{out})$ ,  $b_n(\text{out})$  of out-antineutrinos, the corresponding out-vacuum being  $|0, \text{out}\rangle$ .

Thus for any quantum number  $n$ , we have

$$\begin{aligned} a_n(\text{in})|0, \text{in}\rangle &= b_n(\text{in})|0, \text{in}\rangle = 0, \\ a_n(\text{out})|0, \text{out}\rangle &= b_n(\text{out})|0, \text{out}\rangle = 0. \end{aligned} \quad (3.8)$$

In both cases, by  $n = (\mathbf{p}, \sigma)$  we denote complete sets of quantum numbers that describe both in- and out- particles and antiparticles. The in-operators obey the canonical anticommutation relations,

$$[a_n(\text{in}), a_{n'}^\dagger(\text{in})]_+ = [b_n(\text{in}), b_{n'}^\dagger(\text{in})]_+ = \delta_{n, n'}. \quad (3.9)$$

All other anticommutators between the in-operators are equal to zero. The out-operators obey similar anticommutation relations,

$$\begin{aligned} [a_n(\text{out}), a_{n'}^\dagger(\text{out})]_+ &= [b_n(\text{out}), b_{n'}^\dagger(\text{out})]_+ \\ &= \delta_{n, n'}, \end{aligned} \quad (3.10)$$

and all other anticommutators between the out-operators also are equal to zero.

The above in- and out-operators are defined by two decompositions of the quantum Dirac field  $\Psi(X)$  in the exact solutions of the Dirac equation,

$$\begin{aligned} \Psi(X) &= \sum_n [a_n(\text{in}) + \psi_n(X) + b_n^\dagger(\text{in}) - \psi_n(X)] \\ &= \sum_n [a_n(\text{out}) + \psi_n(X) \\ &\quad + b_n^\dagger(\text{out}) - \psi_n(X)]. \end{aligned} \quad (3.11)$$

We see that the in-operators are associated with a complete orthonormal set of solutions  $\{\zeta \psi_n(X)\}$  (in the following we shall call it the in-set) of Eq. (2.9) with the effective potential  $g(t)$ , where  $\zeta = +$  stays for neutrinos and  $\zeta = -$  for antineutrinos. Their asymptotics at  $t < t_1$  are wave functions of free particles in the presence of a constant effective potential  $g_1$  and can be classified as neutrino and antineutrino wave functions. The out-operators are associated with another complete orthonormal out-set of solutions  $\{\zeta \psi_n(X)\}$  of Eq. (2.9). Their asymptotics at  $t > t_2$  are wave functions of free particles in the presence of a constant effective potential  $g_2$  and can be classified as neutrino and antineutrino wave functions. The functions  $\zeta \psi_n(X)$  are eigenvectors of the one particle Dirac Hamiltonian  $H(t)$  at  $t = t_1$ ,

$$H(t_1) \zeta \psi_n(t_1, \mathbf{x}) = \zeta \mathcal{E}_1 \zeta \psi_n(t_1, \mathbf{x}), \quad (3.12)$$

where  $\mathcal{E}_1$  are the kinetic energies of in-particles (neutrino or antineutrino) in a state specified by a complete set of quantum numbers  $n$ . The out-particles (neutrino or antineutrino) are associated with a complete out-set of solutions  $\{\zeta \psi_n(X)\}$  of the Dirac equation with the asymptotics  $\zeta \psi_n(t_2, \mathbf{x})$  at  $t_2$  being eigenvectors of the one particle Dirac Hamiltonian at  $t_2$ , namely,

$$H(t_2) \zeta \psi_n(t_2, \mathbf{x}) = \zeta \mathcal{E}_2 \zeta \psi_n(t_2, \mathbf{x}), \quad (3.13)$$

where  $\mathcal{E}_2$  are the kinetic energies of out-particles in a state specified by a complete set of quantum numbers  $n$ .

One can find that for in- and out-sets, the following dispersion relations and the orthonormality conditions hold:

$$\begin{aligned} \mathcal{E}_{1,2} &= \sqrt{m^2 + \left(p - \sigma \frac{g_{1,2}}{2}\right)^2}, \\ (\zeta \psi_n, \zeta' \psi_{n'}) &= \delta_{\zeta, \zeta'} \delta_{\sigma \sigma'} \delta^{(3)}(\mathbf{p} - \mathbf{p}'), \\ (\zeta \psi_n, \zeta' \psi_{n'}) &= \delta_{\zeta, \zeta'} \delta_{\sigma \sigma'} \delta^{(3)}(\mathbf{p} - \mathbf{p}'). \end{aligned} \quad (3.14)$$

It should be noted, that in the following we will use the standard volume regularization:  $\delta(\mathbf{p} - \mathbf{p}') \rightarrow \delta_{\mathbf{p}, \mathbf{p}'}$  and  $\delta_{n, n'} = \delta_{\sigma \sigma'} \delta_{\mathbf{p}, \mathbf{p}'}$ . Accounting for the orthonormality relations in Eq. (3.14) and the completeness of the in- and out- sets, one can demonstrate that anticommutation relations in Eqs. (3.9) and (3.10) for the introduced creation and annihilation in- or out-operators match with

equal time anticommutation relations for the Heisenberg operators in Eq. (3.5).

Being expressed in terms of the creation and annihilation operators, the operators of physical quantities given by Eqs. (3.6) and (3.7) take the form

$$\begin{aligned}
\hat{H}(t_1) &= \sum_n \mathcal{E}_1 [a_n^\dagger(\text{in}) a_n(\text{in}) + b_n^\dagger(\text{in}) b_n(\text{in})], \\
H_0(t_1) &= \sum_n \mathcal{E}_1, \\
\hat{H}(t_2) &= \sum_n \mathcal{E}_2 [a_n^\dagger(\text{out}) a_n(\text{out}) + b_n^\dagger(\text{out}) b_n(\text{out})], \\
H_0(t_2) &= \sum_n \mathcal{E}_2, \\
\hat{\mathbf{p}} &= \sum_n \mathbf{p} [a_n^\dagger(\text{in}) a_n(\text{in}) - b_n^\dagger(\text{in}) b_n(\text{in})] \\
&= \sum_n \mathbf{p} [a_n^\dagger(\text{out}) a_n(\text{out}) - b_n^\dagger(\text{out}) b_n(\text{out})], \\
\hat{\Xi} &= \sum_n \sigma [a_n^\dagger(\text{in}) a_n(\text{in}) - b_n^\dagger(\text{in}) b_n(\text{in})] \\
&= \sum_n \sigma [a_n^\dagger(\text{out}) a_n(\text{out}) \\
&\quad - b_n^\dagger(\text{out}) b_n(\text{out})]. \tag{3.15}
\end{aligned}$$

We see that the creation and annihilation operators diagonalize the kinetic energy operators  $\hat{H}(t_1)$  and  $\hat{H}(t_2)$ , which are positive defined. It confirms the interpretation of the operators  $a_n^\dagger(\text{in})$ ,  $a_n(\text{in})$ ,  $a_n^\dagger(\text{out})$ , and  $a_n(\text{out})$  as well as  $b_n^\dagger(\text{in})$ ,  $b_n(\text{in})$ ,  $b_n^\dagger(\text{out})$ , and  $b_n(\text{out})$  as describing a neutrino and an antineutrino at  $t = t_1$  and  $t = t_2$ .

As was already mentioned above, the operators  $\hat{\mathbf{p}}$  and  $\hat{\Xi}$  are the integrals of motion and are diagonal in both in- and out-particle operators. Using the representations in Eq. (3.15), one can establish relations between quantum numbers  $\mathbf{p}$ ,  $\sigma$  and corresponding physical quantities. Namely, the physical momentum of in- and out-neutrino is  $\mathbf{p}_{\text{ph}} = \mathbf{p}$  and the physical helicity is  $\sigma_{\text{ph}} = \sigma$ , whereas  $\mathbf{p}_{\text{ph}} = -\mathbf{p}$  and  $\sigma_{\text{ph}} = -\sigma$  for in- and out-antineutrino. The one-particle definition of the physical helicity operator is  $\Xi_{\mathbf{p}}^{\text{ph}} = \frac{\mathbf{p}_{\text{ph}} \cdot \boldsymbol{\Sigma}}{p_{\text{ph}}}$  for states of both neutrinos and antineutrinos with a given momenta. It is consistent with the above given physical interpretation of the quantum numbers  $\mathbf{p}$  and  $\sigma$  if one takes into account that  $\Xi_{\mathbf{p}}^{\text{ph}} = \mathbf{p} \cdot \boldsymbol{\Sigma} / p$  for neutrino, whereas  $\Xi_{\mathbf{p}}^{\text{ph}} = -\mathbf{p} \cdot \boldsymbol{\Sigma} / p$  for antineutrino.

Further, we will see that neutrinos and antineutrinos created or annihilated from/to the vacuum have the same quantum numbers  $\mathbf{p}$  and  $\sigma$  due to conservation law. This means that neutrinos and antineutrinos are produced or annihilated with opposite physical momenta and helicities. This matches with the interpretation given above in Sec. III A.

In- and out-solutions with given quantum numbers  $n$

are related by linear transformations of the form

$$\begin{aligned}
\zeta \psi_n(X) &= G(+|\zeta) \psi_n(X) + G(-|\zeta) \bar{\psi}_n(X), \\
\zeta \bar{\psi}_n(X) &= G(+|\zeta) \bar{\psi}_n(X) \\
&\quad + G(-|\zeta) \psi_n(X), \tag{3.16}
\end{aligned}$$

where coefficients  $G$  are defined via the inner products of these sets,

$$\begin{aligned}
(\zeta \psi_{n'}, \zeta' \psi_n) &= \delta_{n,n'} G(\zeta|\zeta'), \\
G(\zeta'|\zeta) &= G(\zeta|\zeta')^*. \tag{3.17}
\end{aligned}$$

These coefficients satisfy the unitarity relations

$$\begin{aligned}
G(\zeta|+) G(+|\zeta) + G(\zeta|-) G(-|\zeta) &= 1, \\
G(\zeta|+) G(+|\zeta) + G(\zeta|-) G(-|\zeta) &= 1, \\
G(+|+) G(+|-) + G(+|-) G(-|-) &= 0, \\
G(+|+) G(+|-) + G(+|-) G(-|-) &= 0, \tag{3.18}
\end{aligned}$$

which follow from the orthonormalization and completeness relations for the corresponding solutions. It is known that all the coefficients can be expressed in terms of two of them, e.g., of  $G(+|+)$  and  $G(-|+)$ . However, even these coefficients are not completely independent,

$$|G(-|+)|^2 + |G(+|+)|^2 = 1. \tag{3.19}$$

A linear canonical transformation (Bogolyubov transformation) between in- and out- operators which can be derived from Eq. (3.11) has the form

$$\begin{aligned}
a_n(\text{out}) &= G(+|+) a_n(\text{in}) + G(+|-) b_n^\dagger(\text{in}), \\
b_n^\dagger(\text{out}) &= G(-|+) a_n(\text{in}) + G(-|-) b_n^\dagger(\text{in}). \tag{3.20}
\end{aligned}$$

All the information about neutrino and antineutrino creation, annihilation, and scattering in a background matter can be extracted from the coefficients  $G(\zeta|\zeta')$ . For example, using Eq. (3.20), we find the differential mean number  $N_n$  of neutrino or antineutrino created (which are also equal to the mean number of  $\nu\bar{\nu}$  pairs created) from the in-vacuum with a given momentum  $\mathbf{p}$  and spin projection  $\sigma$  is

$$N_n = \langle 0, \text{in} | a_n^\dagger(\text{out}) a_n(\text{out}) | 0, \text{in} \rangle = |G(-|+)|^2. \tag{3.21}$$

The total number  $\mathcal{N}_\sigma$  of created  $\nu\bar{\nu}$  pairs with a given  $\sigma$  is the sum over all the momenta,

$$\mathcal{N}_\sigma = \sum_{\mathbf{p}} N_n = \frac{V}{(2\pi)^3} \int N_n d\mathbf{p}. \tag{3.22}$$

The probability of the neutrino scattering  $P(+|+)_{n,n'}$  and the probability of a pair creation  $P(-|0)_{n,n'}$  are,

respectively

$$\begin{aligned}
P(+|+)_{n,n'} &= |\langle 0, \text{out} | a_n(\text{out}) a_{n'}^\dagger(\text{in}) | 0, \text{in} \rangle|^2 \\
&= \delta_{n,n'} \frac{1}{1 - N_n} P_v, \\
P(-+|0)_{n,n'} &= |\langle 0, \text{out} | b_n(\text{out}) a_{n'}(\text{out}) | 0, \text{in} \rangle|^2 \\
&= \delta_{n,n'} \frac{N_n}{1 - N_n} P_v. \quad (3.23)
\end{aligned}$$

The probability for the neutrino vacuum to remain a vacuum reads

$$P_v = |\langle 0, \text{out} | 0, \text{in} \rangle|^2 = \exp \left\{ \sum_{\sigma, \mathbf{p}} \ln(1 - N_n) \right\}. \quad (3.24)$$

The probabilities for an antineutrino scattering and a  $\nu\bar{\nu}$  pair annihilation are given by the same expressions  $P(+|+)$  and  $P(-+|0)$ , respectively.

In the general case, states of the system under consideration at the final time instant contain particles and antiparticles due to the  $\nu\bar{\nu}$  pair creation from the vacuum and due to the possible existence of some particles and antiparticles (we call them initial in what follows) in the initial state of the system. It was found in Ref. [4] that the following relation holds true:

$$\begin{aligned}
\aleph_n^{(\zeta)}(\text{out}) &= (1 - N_n) \aleph_n^{(\zeta)}(\text{in}) \\
&+ N_n \left[ 1 - \aleph_n^{(-\zeta)}(\text{in}) \right], \quad (3.25)
\end{aligned}$$

where  $\aleph_n^{(\zeta)}(\text{in})$  and  $\aleph_n^{(\zeta)}(\text{out})$  are initial and the final differential mean numbers of particles ( $\zeta = +$ ) and antiparticles ( $\zeta = -$ ). Here  $N_n$  is given by Eq. (3.21). Thus, if the initial state differs from the vacuum, the differential mean numbers of neutrinos or antineutrinos created by the effective potential  $g(t)$  are given by the difference  $\Delta \aleph_n^{(\zeta)} = \aleph_n^{(\zeta)}(\text{out}) - \aleph_n^{(\zeta)}(\text{in})$ .

Using Eq. (3.25), we obtain that

$$\begin{aligned}
\Delta \aleph_n^{(+)} &= \Delta \aleph_n^{(-)} = \Delta \aleph_n, \\
\Delta \aleph_n &= N_n \left[ 1 - \left( \aleph_n^{(+)}(\text{in}) + \aleph_n^{(-)}(\text{in}) \right) \right]. \quad (3.26)
\end{aligned}$$

Even if  $N_n \neq 0$ , no creation of  $\nu\bar{\nu}$ -pairs with quantum numbers  $n$  occurs provided that  $N_n^{(+)}(\text{in}) + N_n^{(-)}(\text{in}) = 1$ . It happens because of the Pauli blocking when both particle and antiparticle are involved. The  $\nu\bar{\nu}$  pairs creation takes place if  $N_n^{(+)}(\text{in}) + N_n^{(-)}(\text{in}) < 1$ . The annihilation of  $\nu\bar{\nu}$  pairs is possible if  $N_n^{(+)}(\text{in}) + N_n^{(-)}(\text{in}) > 1$ .

#### IV. NEUTRINO CREATION BY A SLOWLY VARYING EFFECTIVE POTENTIAL

In this section we study creation of  $\nu\bar{\nu}$  pairs of various neutrino flavors by a background matter with a linearly growing effective potential. We consider the so-called strong field case, when the difference  $|g(t_{\text{out}})| - |g(t_{\text{in}})|$

between the initial and final potential is greater than the neutrino mass  $m$ . In this sense, one can say that an effective potential  $g(t)$  is slowly varying.

To find all necessary ingredients for calculating the particle-creation effect, we first represent solutions  $\psi(X)$  of Eq. (2.9) in the following form,

$$\psi_n(X) = [i\partial_0 + H(t)] \varphi_{n,\chi}(t) e^{i\mathbf{p}\mathbf{r}} U_{\sigma,\chi}, \quad (4.1)$$

where  $\varphi_{n,\chi}(t)$  are time-dependent scalar functions that satisfy the equation

$$\begin{aligned}
\left[ \frac{d^2}{dt^2} + \left( p - \frac{g(t)}{2} \right)^2 + \frac{i}{2} \chi \partial_t g(t) + m^2 \right] \\
\times \varphi_{n,\chi}(t) = 0, \quad (4.2)
\end{aligned}$$

whereas constant spinors  $U_{\sigma,\chi}$  satisfy the equations

$$\begin{aligned}
\frac{\mathbf{p}\Sigma}{p} U_{\sigma,\chi} &= \sigma U_{\sigma,\chi}, \quad \sigma = \pm 1; \\
\gamma^5 U_{\sigma,\chi} &= \chi U_{\sigma,\chi}, \quad \chi = \pm 1. \quad (4.3)
\end{aligned}$$

Note that  $\gamma^5$  does not commute with the projection operator in the representation given in Eq. (4.1). Therefore solutions  $\psi_n(X)$  that correspond to different spinors  $U_{\sigma,+1}$  and  $U_{\sigma,-1}$  are linear dependent. Then one can choose, for example, either  $\chi = +1$  or  $\chi = -1$ .

Using Eq. (4.1), we express the inner product (2.11) of two arbitrary solutions  $\tilde{\psi}_n(X)$  and  $\tilde{\psi}'_n(X)$  as follows

$$\begin{aligned}
(\psi_n, \psi'_{n'}) &= \delta_{n,n'} V J, \\
J &= U_{\sigma,\chi}^\dagger \varphi_{n,\chi}^*(t) \left( -i \overleftarrow{\partial}_0 + i\partial_0 \right) \\
&\times \left[ i\partial_0 + \chi \left( p\sigma - \frac{g(t)}{2} \right) + m\gamma^0 \right] \\
&\times \varphi'_{n,\chi}(t) U_{\sigma,\chi}. \quad (4.4)
\end{aligned}$$

Then, we obtain the quantity  $J$  in the following form

$$\begin{aligned}
J &= \delta_{n,n'} \varphi_{n,\chi}^*(t) \left( -i \overleftarrow{\partial}_0 + i\partial_0 \right) \\
&\times \left[ i\partial_0 + \chi \left( p\sigma - \frac{g(t)}{2} \right) \right] \varphi'_{n,\chi}(t). \quad (4.5)
\end{aligned}$$

Setting  $t = t_1$  and  $t = t_2$  in Eqs. (3.12), (3.13), and (4.4), one gets that particle and antiparticle degrees of freedom are simultaneously orthogonal:  $(+\psi_n, -\psi_{n'}) = (+\psi_n, -\psi_{n'}) = 0$ . We see that here it is enough to know only scalar functions in Eq. (4.1). The same holds true for the calculation of all other necessary quantities.

Now we consider the case of a slowly varying effective potential supposing that  $g(t)$  is a linear function in a rather big time interval  $T = t_2 - t_1$ . Namely, we are going to consider the following time dependence of effective potential,

$$g(t) = \begin{cases} g_1, & t < t_1, \\ b - at, & t_1 \leq t \leq t_2, \\ g_2, & t > t_2, \end{cases} \quad (4.6)$$

where  $g(t_1) = g_1$  and  $g(t_2) = g_2$  are constant values and

$$a = -\frac{g_2 - g_1}{t_2 - t_1} \neq 0, \quad b = \frac{g_1 t_2 - g_2 t_1}{t_2 - t_1}. \quad (4.7)$$

We shall study the  $\nu\bar{\nu}$  pairs creation due to the compression before the hydrodynamic bounce which happens during  $0.10\text{ s} \lesssim t \lesssim 0.11\text{ s}$  ( $t = 0$  corresponds to the beginning of the collapse) and during the neutronization of PNS which occurs during  $0.11\text{ s} \lesssim t \lesssim 0.12\text{ s}$  (for the details see Ref. [25] and Sec. V). If we study the pairs creation due to the matter compression in the PNS core, using Eqs. (2.5) and (2.7), we obtain, for example, that  $g_1 = g(t_{\text{in}}) \approx 0$  for all the neutrino flavors, whereas  $g_2 = g(t_{\text{out}}) = 0$  for  $\nu_e$  and  $g_2 = g(t_{\text{out}}) < 0$  for  $\nu_\mu, \nu_\tau$ . If we examine the vacuum instability in the neutronization of PNS that occurs outside the core, then  $g_2 = g(t_{\text{out}}) < 0$  for all the neutrino flavors. However  $g_1 = g(t_{\text{in}}) > 0$  for  $\nu_e$  and  $g_1 = g(t_{\text{in}}) < 0$  for  $\nu_\mu$  and  $\nu_\tau$ . We can always choose  $t_{1,2}$  to have  $b = 0$  in Eq. (4.7). The model with the external field  $g(t)$  given by Eq. (4.6) is technically similar to the QED model with the  $T$ -constant external electric field studied in Ref. [22] and can be treated similarly.

First of all, we consider solutions in Eq. (4.1) at  $t < t_1$  and  $t > t_2$  corresponding to the constant effective potential  $g_1$  or  $g_2$ , respectively. We present such solutions in the following normalized form

$$\begin{aligned} \zeta \psi_n(X) &= [i\partial_0 + H(t)] \zeta \varphi_{n,\chi}(t) e^{i\mathbf{p}\mathbf{r}} U_{\sigma,\chi}, \\ \zeta \varphi_{n,\chi}(t) &= C_1^\zeta \exp[-i\zeta \mathcal{E}_1(t - t_1)], \quad t < t_1, \\ \zeta \psi_n(X) &= [i\partial_0 + H(t)] \zeta \varphi_{n,\chi}(t) e^{i\mathbf{p}\mathbf{r}} U_{\sigma,\chi}, \\ \zeta \varphi_{n,\chi}(t) &= C_2^\zeta \exp[-i\zeta \mathcal{E}_2(t - t_2)], \quad t > t_2, \\ C_{1,2}^\zeta &= (2V\mathcal{E}_{1,2})^{-1/2} \left| \mathcal{E}_{1,2} - \zeta \chi \left( \frac{g_{1,2}}{2} - \sigma p \right) \right|^{-1/2} \end{aligned} \quad (4.8)$$

where neutrino and antineutrino states are identified according to the kinetic energy signs in Eqs. (3.12) and (3.13). Normalization factors  $C_{1,2}^\zeta$  are calculated in accordance with Eqs. (4.4) and (4.5).

Using representations in Eq. (4.8), we can reproduce solutions of the Dirac equation obtained in Sec. III A.

Indeed, let us write

$$\varphi_{n,\chi} \sim \exp(\mp i\mathcal{E}_{1,2}t + i\mathbf{p}\mathbf{r}), \quad U_{\sigma,\chi} \sim \begin{pmatrix} w_\sigma \\ \chi w_\sigma \end{pmatrix}. \quad (4.9)$$

Using the explicit form of  $\gamma$  matrices in Eq. (2.2) one can verify that Eq. (4.3) holds true. Then we see that, for  $\chi = +1$ , the corresponding neutrino wave functions  $\psi_n(X) \exp(-itg_{1,2}/2)$  coincide with the function given by Eqs. (3.2) and (3.3) up to constant factors. Thus, neutrino wave functions considered in Sec. III A are consistent with wave functions that are obtained for time-dependent effective potentials (see also Ref. [20]).

Now, we consider solutions (4.1) at  $t_1 \leq t \leq t_2$ . In this time region, the functions  $\varphi_{n,\chi}(t)$  satisfy the following equation:

$$\left[ \frac{d^2}{d\xi^2} + \xi^2 - i\chi \text{sgn}(a) + \lambda \right] \varphi_{n,\chi}(t) = 0, \quad (4.10)$$

where  $\lambda = 2m^2/|a|$  and

$$\xi = \sqrt{\frac{2}{|a|}} \left( \frac{a}{2}t - \frac{b}{2} + \sigma p \right) \text{sgn}(a). \quad (4.11)$$

For  $\chi \text{sgn}(a) = +1$ , one can see that two independent solutions of Eq. (4.10) are  $D_\rho[(1-i)\xi]$  and  $D_{-1-\rho}[(1+i)\xi]$ , where  $D_\rho(\xi)$  is Weber parabolic cylinder function (WPCF) and  $\rho = i\lambda/2$ . It is known that these solutions form a complete set. Some useful properties of these solutions are summarized in Appendix B and will be used in what follows.

To obtain the coefficient  $G(-|+)$ , corresponding to the time-dependent effective potential in Eq. (4.6), we use Eq. (4.5). Since the inner product in Eq. (4.4) is time independent we can use any convenient time instant for its calculation. Let us set  $t = t_0 < t_1$  in Eq. (4.5). Then we have to use the corresponding functions  $-\varphi_{n,\chi}(t)$  from Eq. (4.8). According to Eq. (3.16) the function  $+\varphi_{n,\chi}(t)$  for any time instant can be presented in the form

$$+\varphi_{n,\chi}(t) = \begin{cases} G(+|+)\varphi_{n,\chi}(t) + G(-|+)\varphi_{n,\chi}(t), & t < t_1, \\ C_2^+ (d_1 D_\rho[(1-i)\xi] + d_2 D_{-1-\rho}[(1+i)\xi]), & t_1 \leq t \leq t_2, \\ C_2^+ \exp[-i\mathcal{E}_2(t - t_2)], & t > t_2. \end{cases} \quad (4.12)$$

The coefficients  $d_{1,2}$  will be specified below. The functions  $+\varphi_{n,\chi}(t)$  and their derivatives  $\partial_t +\varphi_{n,\chi}(t)$  satisfy

the following gluing conditions:

$$\begin{aligned} +\varphi_{n,\chi}(t_k - 0) &= +\varphi_{n,\chi}(t)(t_k + 0), \\ \partial_t +\varphi_{n,\chi}(t_k - 0) &= \partial_t +\varphi_{n,\chi}(t)(t_k + 0), \\ k &= 1, 2. \end{aligned} \quad (4.13)$$

Let us choose, for example,  $\chi \text{sgn}(a) = +1$ . Then, at



$t = t_2$ , it follows from Eq. (4.13) that

$$d_{1,2} = \mp \frac{\mathcal{E}_2}{\sqrt{a} \exp[(\lambda - i)\pi/4]} f_{1,2}(t_2), \quad (4.14)$$

where

$$\begin{aligned} f_1(t) &= \left\{ 1 - \frac{i}{\sqrt{\xi^2 + \lambda}} \frac{d}{d\xi} \right\} D_{-1-i\lambda/2}[(1+i)\xi], \\ f_2(t) &= \left\{ 1 - \frac{i}{\sqrt{\xi^2 + \lambda}} \frac{d}{d\xi} \right\} D_{i\lambda/2}[(1-i)\xi]. \end{aligned} \quad (4.15)$$

Finally, applying Eq. (4.13) at  $t = t_1$ , we get  $G(-|+)$  in the following form:

$$\begin{aligned} G(-|+) &= \exp[-(\lambda - i)\pi/4] AB, \\ B &= [f_1(t_1)f_2(t_2) - f_2(t_1)f_1(t_2)], \\ A &= \left[ \frac{\sqrt{\xi_1^2 + \lambda} \sqrt{\xi_2^2 + \lambda} (\sqrt{\xi_1^2 + \lambda} - \xi_1)}{8\sqrt{\xi_2^2 + \lambda} + \xi_2} \right]^{1/2} \end{aligned} \quad (4.16)$$

where

$$\xi_{1,2} = \xi|_{t=t_{1,2}} = \sqrt{\frac{2}{|a|}} \left( \sigma p - \frac{g_{1,2}}{2} \right) \text{sgn}(a), \quad (4.17)$$

According to Eq. (3.21), the differential mean numbers of the  $\nu\bar{\nu}$  pairs created by the effective potential Eq. (4.6) are

$$N_n = |G(-|+)|^2 = e^{-\pi\lambda/2} A^2 |B|^2. \quad (4.18)$$

They depend only on the values  $\xi_{1,2}$  for a given  $\lambda$ . Similar expressions were obtained in Ref. [22] in the problem of particle creation by a quasiconstant uniform electric field.

We are interested in the case of a slowly varying strong effective potential  $g(t)$ , that satisfies the condition

$$\begin{aligned} |g_2 - g_1| |a|^{-1/2} &= [|g_2 - g_1| (t_2 - t_1)]^{1/2} \\ &\gg K \gg \max\{1, \lambda\}, \end{aligned} \quad (4.19)$$

where  $K$  is a given number. The case when both  $|\xi_1|$  and  $|\xi_2|$  are sufficiently large,

$$|\xi_{1,2}| \geq K \gg \max\{1, \lambda\}, \quad (4.20)$$

is only possible when signs of  $\xi_1$  and  $\xi_2$  are opposite. In this case, using asymptotic expansions of WPCF, we obtain (see details in Appendix B) that

$$N_n = e^{-\pi\lambda} \left[ 1 + O(|\xi_1|^{-3}) + O(|\xi_2|^{-3}) \right]. \quad (4.21)$$

Consequently, the quantity (4.21) is almost constant over the wide range of momenta if Eq. (4.20) holds true. For the case of sufficiently big momenta, when  $\xi_1 \approx \xi_2$ , we find that the quantity  $N_n$  is very small,

$$\begin{aligned} N_n &\sim \max\left\{ |\xi_1|^{-6}, |\xi_2|^{-6} \right\} \quad \text{if} \\ &\min\{|\xi_1|, |\xi_2|\} \geq K. \end{aligned} \quad (4.22)$$

In the intermediate region the values of  $|\xi_1|$  and  $|\xi_2|$  are quite different. For example, when  $|\xi_2| \geq K$  then  $|\xi_1| < K$  and vice versa. Thus, here, we cannot use any asymptotic expansion of WPCFs to analyze the  $\xi_1$ -dependence of  $N_n$ . However, one can make some conclusions about the contribution of this region to the integral over the momenta in Eqs. (3.22). Taking into account that  $N_n$  is always smaller than one for fermions, one can get a rough estimation

$$\begin{aligned} \int_{|\xi_1| < K} N_n dp &< \int_{|\xi_1| < K} dp \\ &\sim V \max \left\{ \sqrt{|a|} K |g_1|^2, \left( \sqrt{|a|} K \right)^3 \right\}. \end{aligned}$$

A more accurate estimations can be made numerically. We assume that  $\xi_2 \geq K$  and  $|\xi_1| < K$ . Using the only asymptotics with respect to  $\xi_2$  given by Eq. (B4) and the exact form of  $f_1(t_1)$  given by Eq. (4.15), we find that

$$\begin{aligned} N_n &= \frac{1}{4} e^{-\pi\lambda/4} \sqrt{\xi_1^2 + \lambda} \\ &\times \left( \sqrt{\xi_1^2 + \lambda} - \xi_1 \right) |f_1(t_1)|^2, \end{aligned} \quad (4.23)$$

exactly in  $\xi_1$ . The dependence on  $\xi_1$  of  $N_n$  given by Eq. (4.23) is made numerically for different  $\lambda$  and is presented on Fig. 1. Thus, we find that the contribution from the intermediate region to the integral in Eq. (3.22) is much less than that given by a rough estimate. In particular, we show that the value  $K = 3$  is sufficiently large for the problem in question.

Thus, the parameter  $K$  plays the role of a sharp cutoff in the integral in Eq. (3.22). Finally we find that the differential mean numbers of neutrinos or antineutrinos can be written as

$$N_n = \begin{cases} e^{-\pi\lambda}, & \mathbf{p} \in D_\sigma \\ 0, & \mathbf{p} \notin D_\sigma \end{cases}, \quad (4.24)$$

where

$$\begin{aligned} D_\sigma : |\xi_{1,2}| &\geq K \gg \max\{1, \lambda\}, \\ \text{sgn}(\xi_1) &= -\text{sgn}(\xi_2). \end{aligned} \quad (4.25)$$

We see that in the range  $D_\sigma$  the distribution  $N_n$  is uniform and rotationally invariant and is completely determined by the value of  $\lambda$ .

We can conditionally consider  $\lambda \lesssim 1$  as a characteristic of the strong-field case, and  $\lambda \gg 1$  as a characteristic of the weak-field case. The effect of particle creation is negligible small in the latter case. Here we have similar situation with the charged particle creation by an electric field  $E$  from the vacuum, where there exists similar parameter  $m^2/eE$  and its characteristic value  $m^2/eE = 1$  defines the Schwinger's critical field  $E_{\text{cr}} = m^2/e$ .

In the following we assume that in our problem  $\lambda \lesssim 1$  and define the critical neutrino mass  $m^{(\text{cr})}$  from the condition  $\lambda = 1$ . Obviously, the effect of neutrino creation

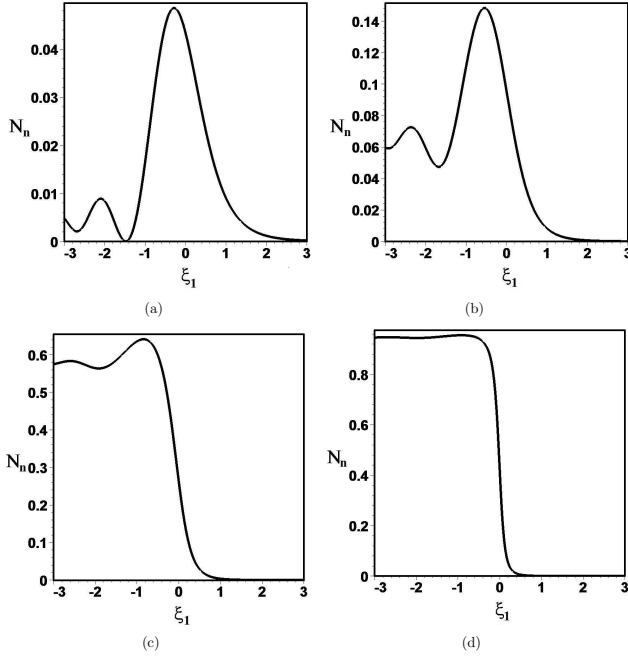


FIG. 1. The dependence of the number of  $N_n$  in Eq. (4.23) versus  $\xi_1$  for different  $\lambda$ . The panel (a) corresponds to  $\lambda = 2$ , the panel (b) – to  $\lambda = 1$ , the panel (c) – to  $\lambda = 0.2$ , and the panel (d) – to  $\lambda = 0.02$ .

can be in principle observed if there exists a kind of neutrinos with masses that are less or comparable with such a critical mass. For the further estimations, it is convenient, using the definition of  $a$  in Eq. (4.7), to express  $\lambda$  as follows

$$\lambda = \frac{2m^2(t_2 - t_1)}{|g_2 - g_1|}. \quad (4.26)$$

The total number  $\mathcal{N}_\sigma$  of neutrino or antineutrino with a given  $\sigma$  created from vacuum is proportional to the total number of states  $\Delta_\sigma$  with the neutrino momenta that belong to the range  $D_\sigma$ . Thus, we have

$$\mathcal{N}_\sigma = e^{-\pi\lambda} \Delta_\sigma, \quad \Delta_\sigma = \frac{V}{(2\pi)^3} \int_{D_\sigma} d\mathbf{p}. \quad (4.27)$$

The logarithm of the probability for the neutrino vacuum to remain a vacuum given by Eq. (3.24) is also proportional to  $\Delta_\sigma$ ,

$$\ln P_v = \ln(1 - e^{-\pi\lambda}) (\Delta_{+1} + \Delta_{-1}). \quad (4.28)$$

Note that if  $e^{-\pi\lambda} \ll 1$  then  $\ln P_v \approx -(\mathcal{N}_{+1} + \mathcal{N}_{-1})$ .

The energy density of created neutrino or antineutrino with a given  $\sigma$  has the form

$$w_\sigma = \frac{e^{-\pi\lambda}}{(2\pi)^3} \int_{D_\sigma} \mathcal{E}_2 d\mathbf{p}, \quad (4.29)$$

where  $\mathcal{E}_2$  is defined by Eq. (3.14). In the strong-field case defined just above, the dependence on the cutoff  $K$  can be ignored in Eqs. (4.27)-(4.29).

Considering other models with slowly varying effective potentials that correspond to the strong field case, cf. Ref. [22], one can verify that effects of switching on and off do not change essentially the form of the distribution (4.24) if some conditions similar to the one (4.19) are fulfilled.

As was mentioned in Sec. II, we suppose that transitions between eigenstates that correspond to different neutrino flavors are suppressed. In such a case, we suppose that there exist three effective masses  $m_{\nu_e}$ ,  $m_{\nu_\mu}$ , and  $m_{\nu_\tau}$  of three active neutrino flavors  $\nu_e$ ,  $\nu_\mu$ , and  $\nu_\tau$ . Of course, all the results obtained above for a single mass  $m$  hold true for each mass  $m = m_\alpha$ , where  $\alpha = \nu_e, \mu, \tau$ . Since the problem of the neutrino masses hierarchy is still an open question [23], any one of these masses can be critical. That is why we have to consider all the possibilities. We denote the parameters (4.26) by  $\lambda_e$ ,  $\lambda_\mu$ , and  $\lambda_\tau$  for  $m_{\nu_e}$ ,  $m_{\nu_\mu}$ , and  $m_{\nu_\tau}$  respectively.

The difference in the effective potentials for  $\nu_e$  and  $\nu_{\mu,\tau}$  in Eq. (2.5) implies the difference in the momentum ranges of the corresponding neutrinos created at the neutronization stage. We assume that  $a > 0$ . Then, e.g. it results from Eq. (2.7) that  $g_1 = g(t_{\text{in}}) > 0$  and  $g_2 = g(t_{\text{out}}) = -2g(t_{\text{in}})$  for  $\nu_e$ . Using Eq. (4.25), we find that the maximal range of  $\nu_e$  momenta is

$$\begin{aligned} D_{-1}^e : p &\leq \frac{|g_2|}{2} - \sqrt{\frac{a}{2}}K \text{ if } \sigma = -1, \\ D_{+1}^e : p &\leq \frac{g_1}{2} - \sqrt{\frac{a}{2}}K \text{ if } \sigma = +1. \end{aligned} \quad (4.30)$$

We see that it depends on the neutrino helicity.

The total number of states  $\Delta_\sigma^e$  in the range given by Eq. (4.25) can be considered as the function of the interval  $T = t_2 - t_1$  of the effective potential variation. Note that one can take any value of  $g_1 \geq g(t_{\text{in}})$  as initial and  $g_2 \leq g(t_{\text{out}})$  as final unless the condition (4.19) is fulfilled for these quantities. Then specific intervals of a pair formation can be determined. In particular, one can find ranges of the momenta for the  $\nu_e$  created before the value  $g(t)$  decreases to zero at some time  $t_0$  ( $g(t) > 0$  part) and after that ( $g(t) < 0$  part). In the first situation, one has  $g_1 = g(t_{\text{in}})$  and  $g_2 = 0$ , while in the second,  $g_1 = 0$  and  $g_2 = g(t_{\text{out}})$ . Then not empty ranges are

$$\begin{aligned} D_{-1}^e(g(t) < 0) : \sqrt{\frac{a}{2}}K &\leq p \leq \frac{|g_2|}{2} - \sqrt{\frac{a}{2}}K, \\ \text{for } g(t) < 0, \text{ if } \sigma &= -1, \\ D_{+1}^e(g(t) > 0) : \sqrt{\frac{a}{2}}K &\leq p \leq \frac{g_1}{2} - \sqrt{\frac{a}{2}}K, \\ \text{for } g(t) > 0, \text{ if } \sigma &= +1. \end{aligned} \quad (4.31)$$

We see that the  $\nu_e \bar{\nu}_e$  pairs with  $\sigma = -1$  are mainly created when the potential  $g(t)$  becomes negative, in contrast to the  $\nu_e \bar{\nu}_e$  pairs with  $\sigma = +1$  that are created earlier. Using Eqs. (4.30) and (4.31), we find that the maximal kinetic energy of created electron neutrino or

antineutrino at final time instant of the neutronization  $t = t_{\text{out}}$  reads

$$\max \mathcal{E}_2(t_{\text{out}}) \approx \begin{cases} \frac{1}{2} |g(t_{\text{out}})|, & \text{if } \sigma = -1, \\ \frac{3}{4} |g(t_{\text{out}})|, & \text{if } \sigma = +1. \end{cases}$$

However, during the stage of  $\nu_e \bar{\nu}_e$  pair creation with  $\sigma = +1$ ,  $t < t_0$ , when  $g_2 = g(t) > 0$ , the maximal kinetic energy of created electron neutrino or antineutrino increases as  $\max \mathcal{E}_2(t) \approx \frac{1}{2} [g(t_{\text{in}}) - g(t)]$  and reaches its maximal value  $\max \mathcal{E}_2(t_0) \approx \frac{1}{2} g(t_{\text{in}}) = \frac{1}{4} |g(t_{\text{out}})|$  at the end of this stage. This value of the maximal kinetic energy is consistent with the fact that the rest  $\frac{1}{2} |g(t_{\text{out}})|$  of the final kinetic energy  $\max \mathcal{E}_2(t_{\text{out}})$  of this neutrino is gained due to the acceleration of already existing particle after the time instant  $t_0$ .

Thus, total numbers of states  $\Delta_\sigma^e$  of the electron neutrino with a fixed helicity in the momentum range given by Eqs. (4.30) or (4.31) are

$$\begin{aligned} \Delta_{-1}^e &= \frac{V |g(t_{\text{out}})|^3}{3 (4\pi)^2} \left[ 1 + O\left(\frac{\sqrt{a}K}{|g(t_{\text{out}})|}\right) \right], \\ \Delta_{+1}^e &= \frac{V [g(t_{\text{in}})]^3}{3 (4\pi)^2} \left[ 1 + O\left(\frac{\sqrt{a}K}{g(t_{\text{in}})}\right) \right]. \end{aligned} \quad (4.32)$$

We see that  $\Delta_{-1}^e = 8\Delta_{+1}^e$ . Using Eq. (4.29) and (4.32), we find the energy density of created neutrinos or antineutrinos with a given helicity,

$$\begin{aligned} w_{-1}^e &= \langle \mathcal{E}_{-1}^e \rangle e^{-\pi\lambda_e} \Delta_{-1}^e / V, \\ \langle \mathcal{E}_{-1}^e \rangle &= \frac{1}{8} |g(t_{\text{out}})|, \quad \text{if } \sigma = -1, \\ w_{+1}^e &= \langle \mathcal{E}_{+1}^e \rangle e^{-\pi\lambda_e} \Delta_{+1}^e / V, \\ \langle \mathcal{E}_{+1}^e \rangle &= \frac{11}{16} |g(t_{\text{out}})|, \quad \text{if } \sigma = +1, \end{aligned} \quad (4.33)$$

where  $\langle \mathcal{E}_\sigma^e \rangle$  is the mean energy per an electron neutrino or an antineutrino created. We see that the mean energy  $\langle \mathcal{E}_{-1}^e \rangle$  is much less than  $\langle \mathcal{E}_{+1}^e \rangle$ , though the energy densities of created electron neutrinos with the opposite helicity are of the same order,  $w_{+1}^e = \frac{11}{16} w_{-1}^e$ .

For  $\nu_{\mu,\tau}$  it follows from Eq. (2.7) that  $g_1 = g(t_{\text{in}}) < 0$  and  $g_2 = g(t_{\text{out}}) = +2g(t_{\text{in}})$ . Using Eq. (4.25), we find that in the momentum range

$$D_{-1}^{\mu,\tau} : \frac{|g_1|}{2} + \sqrt{\frac{a}{2}}K \leq p \leq \frac{|g_2|}{2} - \sqrt{\frac{a}{2}}K \quad (4.34)$$

the only  $\nu_{\mu,\tau} \bar{\nu}_{\mu,\tau}$  pairs with  $\sigma = -1$  are created. The maximal kinetic energy of  $\nu_{\mu,\tau}$  or  $\bar{\nu}_{\mu,\tau}$  neutrinos created at final time instant  $t = t_{\text{out}}$  follows from Eq. (4.34) to be  $\max \mathcal{E}_2(t_{\text{out}}) \approx \frac{1}{4} |g(t_{\text{out}})|$ . In the same range, the total number of  $\nu_{\mu,\tau}$  neutrino states with  $\sigma = -1$  has the form

$$\begin{aligned} \Delta_{-1}^{\mu,\tau} &= \left\{ \frac{V \left\{ |g(t_{\text{out}})|^3 - |g(t_{\text{in}})|^3 \right\}}{3 (4\pi)^2} \right\} \\ &\times \left[ 1 + O\left(\frac{\sqrt{a}K}{g(t_{\text{in}})}\right) \right]. \end{aligned} \quad (4.35)$$

The energy density and the mean energy per a particle for created  $\nu_{\mu,\tau} \bar{\nu}_{\mu,\tau}$  are, respectively,

$$\begin{aligned} w_{-1}^{\mu,\tau} &= \langle \mathcal{E}_{-1}^{\mu,\tau} \rangle e^{-\pi\lambda_{\mu,\tau}} \Delta_{-1}^{\mu,\tau} / V, \\ \langle \mathcal{E}_{-1}^{\mu,\tau} \rangle &= \frac{11}{112} |g(t_{\text{out}})|. \end{aligned} \quad (4.36)$$

The effective potential for  $\nu_e$  does not change at the compression stage then there is no  $\nu_e \bar{\nu}_e$  creation. Just as the initial  $g_1 = g(t_{\text{in}}) \approx 0$  and the final  $g_2 = g(t_{\text{out}}) < 0$  for  $\nu_{\mu,\tau}$  at this stage. Using Eq. (4.25), we find that the only  $\nu_{\mu,\tau} \bar{\nu}_{\mu,\tau}$  pairs with  $\sigma = -1$  are created due to the compression and the range of momenta of these pairs is

$$D_{-1}^{\mu,\tau}(c) : \sqrt{\frac{a}{2}}K \leq p \leq \frac{|g_2|}{2} - \sqrt{\frac{a}{2}}K. \quad (4.37)$$

The maximal kinetic energy of created particles at final time instant is  $\max \mathcal{E}_2(t_{\text{out}}) \approx \frac{1}{2} |g(t_{\text{out}})|$  and the total number of states that belong to the range (4.37) is

$$\Delta_{-1}^{\mu,\tau}(c) = \frac{V |g(t_{\text{out}})|^3}{3 (4\pi)^2} \left[ 1 + O\left(\frac{\sqrt{a}K}{|g(t_{\text{out}})|}\right) \right]. \quad (4.38)$$

Then the energy density and the mean energy per a particle for created  $\nu_{\mu,\tau} \bar{\nu}_{\mu,\tau}$  at final time of the compression are, respectively,

$$\begin{aligned} w_{-1}^{\mu,\tau}(c) &= \langle \mathcal{E}_{-1}^{\mu,\tau}(c) \rangle e^{-\pi\lambda_{\mu,\tau}} \Delta_{-1}^{\mu,\tau}(c) / V, \\ \langle \mathcal{E}_{-1}^{\mu,\tau}(c) \rangle &= \frac{1}{8} |g(t_{\text{out}})|. \end{aligned} \quad (4.39)$$

Assuming that  $g_2 = g(t)$  changes from  $g(t_{\text{in}})$  to  $g(t_{\text{out}})$ , one can obtain time dependence of all the physical quantities during the neutronization. Note that the numbers of states  $\Delta_\sigma$  given by Eqs. (4.32), (4.35), and (4.38) are nonlinear functions of the time instants  $t_{\text{out}}$  and  $t_{\text{in}}$ . Therefore the total particle production rate is not a conserved physical quantity in this case.

## V. NEUTRINO CREATION IN REALISTIC ASTROPHYSICAL MEDIA

In this section, in the framework of the above developed technique we study  $\nu\bar{\nu}$  pair creation in realistic astrophysical media. In particular, we consider this effect at the compression stage before the hydrodynamic bounce and at the neutronization of PNS. In both cases we derive the upper limit on neutrino masses that corresponds to the nonvanishing probability of  $\nu\bar{\nu}$  pairs creation. Then we discuss the evolution of the created neutrinos.

It is commonly believed that a star having (10–25) solar masses, ends its evolution as a neutron star through a core-collapsing supernova stage with the emission of 99% of the initial gravitational energy in the form of neutrinos [24].

According to the modern simulations (see, e.g., Ref. [25]) the density in the central part on PNS reaches

$\sim 10^{12} \text{ g} \cdot \text{cm}^{-3}$  at  $\sim 100 \text{ s}$  after the beginning of the collapse. High-energy ( $E \geq 10 \text{ MeV}$ ) neutrinos, which are created in the core of PNS, cannot escape since their mean free path is much less than the core radius. During the next  $T_\nu \approx 10 \text{ ms}$  the central density increases to  $\gtrsim 2 \times 10^{14} \text{ g} \cdot \text{cm}^{-3}$ . At this stage the compression of matter in PNS core stops and the hydrodynamic bounce happens.

The bounce is typically followed by the neutronization of PNS matter. The neutronization is characterized by the change of  $Y_e$  from 0.5 to practically zero value. This process occurs outside the PNS core at  $10 \text{ km} \lesssim r \lesssim 100 \text{ km}$ , begins at  $t \approx 0.11 \text{ s}$ , and lasts  $T_\nu \sim 10^{-2} \text{ s}$  (see, e.g., Ref. [25]). The liberated lepton number is carried away by  $\nu_e$  produced in the reaction  $e^- + p \rightarrow n + \nu_e$  and having the energy  $\sim 10 \text{ MeV}$ .

First let us we discuss the creation of  $\nu\bar{\nu}$  pairs due to the matter compression using our formalism during  $T_\nu = 10 \text{ ms}$  just before the bounce. We should mention that one can neglect the radial hydrodynamic currents directed towards the center of PNS [see Eq. (2.3)] in the effective potential of the neutrino interaction with background fermions. Such a contribution is inevitable since the central density is increasing. Supposing that all background fermions have approximately equal radial velocities  $v_r$  and using Eq. (2.3) we get that  $g_r/g = v_r$ . As found in Ref. [26],  $v_r \lesssim 0.1$  inside the PNS core,  $r \lesssim 10 \text{ km}$ , within the considered time of the PNS evolution. Thus  $g_r$  is much less than  $g$ .

Since the matter density increases two orders of magnitude, we can take that  $g(t_{\text{in}}) \approx 0$ . The electron fraction  $Y_e = n_e/(n_n + n_p)$  changes from  $\sim 0.5$  to  $\sim 0.3$  [26], which corresponds to  $n_n(t_{\text{out}}) \approx 2n_e(t_{\text{out}})$ . Therefore, using Eq. (2.5) we get that  $g(t_{\text{out}}) \approx 0$  for  $\nu_e$ . Thus the creation of  $\nu_e\bar{\nu}_e$  pairs is suppressed at this stage of the PNS evolution.

Again using Eq. (2.5) we get that for  $\nu_{\mu,\tau}$ ,

$$\begin{aligned} g_1 &= g(t_{\text{in}}) = 0, \\ g_2 &= g(t_{\text{out}}) = -G_F n_n(t_{\text{out}})/\sqrt{2}. \end{aligned} \quad (5.1)$$

Therefore  $\Delta g_{\nu_{\mu,\tau}} = |g_1 - g_2| \neq 0$  and the creation of  $\nu_{\mu,\tau}\bar{\nu}_{\mu,\tau}$  pairs is possible. We shall roughly assume that the effective potential changes linearly from zero to  $g_2$ . Thus the results of Sec. IV are valid.

It results from Eqs. (4.24) and (4.26) that the flux of low-energy  $\nu_{\mu,\tau}\bar{\nu}_{\mu,\tau}$  pairs is sizable if  $\lambda_{\nu_{\mu,\tau}} = 2m_{\nu_{\mu,\tau}}^2 T_\nu / \Delta g_{\nu_{\mu,\tau}} \lesssim 1$ . Assuming that  $Y_e \approx 1/3$ ,  $\rho = 2 \times 10^{14} \text{ g} \cdot \text{cm}^{-3}$ , and  $T_\nu = 10^{-2} \text{ s}$ , we get that  $\Delta g_{\nu_{\mu,\tau}} \approx 5 \text{ eV}$ , where we use value of the Fermi constant  $G_F(\hbar c)^{-3} \approx 1.17 \times 10^{-5} \text{ GeV}^{-2}$ . Finally we obtain the constraint on the electron neutrino mass,

$$m_{\nu_{\mu,\tau}} \lesssim m_{\nu_{\mu,\tau}}^{(\text{cr})} = 4.1 \times 10^{-7} \text{ eV}. \quad (5.2)$$

Note that, if the constraint in Eq. (5.2) is fulfilled, the flux of  $\nu_{\mu,\tau}\bar{\nu}_{\mu,\tau}$  pairs is nonvanishing.

It is interesting to mention that, in the considered time interval just before the bounce, high-energy neutrinos are

produced in the PNS core. However these neutrinos are trapped inside the core due to elastic and quasielastic neutrino scattering off background fermions. We predict a nonzero flux of  $\nu_{\mu,\tau}\bar{\nu}_{\mu,\tau}$  pairs having very small energy  $< 10 \text{ eV}$ . These neutrinos are not trapped inside the core. Indeed, using the neutrino scattering cross sections given in Ref. [27], one finds that the mean free path of these particles in background matter with the density  $2 \times 10^{14} \text{ g} \cdot \text{cm}^{-3}$  is about  $10^{10} \text{ km}$ . Therefore one can consider these neutrinos as precursors of neutronization neutrino burst.

Now let us consider the  $\nu\bar{\nu}$  pairs creation during the neutronization of PNS. Since the number densities of various background fermions change, with the total mass density of PNS matter being constant, the effective potential in Eq. (2.5) also changes [see, e.g., Eq. (2.7)] and we may expect that an additional flux of low-energy  $\nu\bar{\nu}$  pairs can be emitted at the neutronization of PNS. Again we shall assume that the effective potential changes linearly.

(i) First we suppose that the electron neutrino mass  $m_{\nu_e}$  is the smallest among the all neutrino masses.

Since  $Y_e$  changes from 0.5 to 0 in the neutronization of PNS, the number densities before and after the neutronization satisfy,  $n_e(t_{\text{in}}) \approx n_n(t_{\text{in}})$  and  $n_n(t_{\text{out}}) = n_n(t_{\text{in}}) + n_e(t_{\text{in}}) \approx 2n_n(t_{\text{in}})$ . Therefore, using Eq. (2.5), we obtain

$$\begin{aligned} g_1 &= g(t_{\text{in}}) = G_F n_n(t_{\text{out}})/(2\sqrt{2}), \\ g_2 &= g(t_{\text{out}}) = -G_F n_n(t_{\text{out}})/\sqrt{2}, \end{aligned} \quad (5.3)$$

such that for the electron neutrino we have  $\Delta g_{\nu_e} = |g_2 - g_1| = \frac{3}{2}|g(t_{\text{out}})|$ .

Requiring the nonvanishing flux of  $\nu_e\bar{\nu}_e$  pairs by imposing  $\lambda_{\nu_e} = 2m_{\nu_e}^2 T_\nu / \Delta g_e \lesssim 1$  [see Eqs. (4.24) and (4.26)], we get the constraint on the electron neutrino mass,

$$m_{\nu_e} \lesssim m_{\nu_e}^{(\text{cr})} = 5.6 \times 10^{-8} \text{ eV}. \quad (5.4)$$

To derive Eq. (5.4) we assume that  $T_\nu = 10^{-2} \text{ s}$  and  $n_n(t_{\text{out}}) \sim 10^{36} \text{ cm}^{-3}$  then  $g(t_{\text{out}}) \approx 0.064 \text{ eV}$ . The latter quantity corresponds to the mass density  $\lesssim 10^{12} \text{ g} \cdot \text{cm}^{-3}$ .

(ii) Now we suppose that the smallest among the all neutrino masses is either  $m_{\nu_\mu}$  or  $m_{\nu_\tau}$ .

The treatment of both muon and tau neutrinos is the same. For  $\nu_\mu$  and  $\nu_\tau$  we get from Eq. (2.7) that unlike the case (i) the initial and final effective potentials are

$$\begin{aligned} g_1 &= g(t_{\text{in}}) = -G_F n_n(t_{\text{out}})/(2\sqrt{2}), \\ g_2 &= g(t_{\text{out}}) = +2g(t_{\text{in}}). \end{aligned} \quad (5.5)$$

Therefore  $\Delta g_{\nu_{\mu,\tau}} = |g_2 - g_1| = \frac{1}{2}|g(t_{\text{out}})|$ . The flux of the low-energy  $\nu_{\mu,\tau}\bar{\nu}_{\mu,\tau}$  pairs is big enough if  $\lambda_{\mu,\tau} = 2m_{\nu_{\mu,\tau}}^2 T_\nu / \Delta g_{\mu,\tau} \lesssim 1$ . Thus, we obtain the constraint on the appropriate muon and tau neutrino masses:

$$m_{\nu_{\mu,\tau}} \lesssim m_{\nu_{\mu,\tau}}^{(\text{cr})} = 1.9 \times 10^{-8} \text{ eV}. \quad (5.6)$$

It should be also noted that the energy of these  $\nu\bar{\nu}$  pairs does not exceed 0.1 eV for all three active neutrino flavors. The dimensionless parameters in Eq. (4.19) are quite large for the cases (i) and (ii) at the neutronization,  $(|g_2 - g_1|T_\nu)^{1/2} \sim 10^6$ , and for the compression,  $\sim 10^7$ . Then this condition is well satisfied for the subcritical masses given by Eqs. (5.2), (5.4), and (5.6).

In Appendix A we analyzed the influence of other factors which can diminish the flux of created  $\nu\bar{\nu}$  pairs or distort their distribution. Among them we considered the possible Pauli blocking of the creation process, the gravitational interaction of the low-energy neutrinos, the influence of the PNS rotation on the pairs propagation, and low-energy pair production by nucleon-nucleon bremsstrahlung. We found that all these processes do not significantly influence the evolution of  $\nu\bar{\nu}$  pairs created if the mass of the neutrino is small enough. The only factor which essentially influences the evolution of  $\nu\bar{\nu}$  pairs created is the difference between the effective density in the region of the creation and in the point outside this region. The high-density region is a potential well for either neutrino or antineutrino depending on the sign of the effective potential. Then part of these particles, depending on the flavor and helicity, are bounded in the PNS while the antineutrinos of any flavor escape the PNS. If the created pairs are  $\nu_e\bar{\nu}_e$  then part of these neutrinos also escape the PNS. A part of escaped neutrinos that have the negative helicity can interact directly with the matter of electrons and baryons. All the escaped antineutrinos have the negative helicity and do not interact directly with the uniform part of the matter consisting of electrons and baryons. Nevertheless, an effective potential barrier of a neutron star can affect them, causing refraction and reflection, and, in particular, change their helicity in course of a reflection.

Additionally, we evaluated the typical flux of neutrino/antineutrino, created in frames of our formalism, from a possible supernova in our Galaxy, which can reach the Earth. We considered pairs emitted during the core compression stage which have  $g(t_{\text{out}}) \sim 10$  eV and the numbers of occupied states  $\Delta_{-1}^{\mu,\tau}(c)$  given by Eq. (4.38) is of the order of  $\frac{V|g(t_{\text{out}})|^3}{3(4\pi)^2} \sim 10^{33}$  for  $R_c \sim 10$  km. Supposing that the distance to a supernova  $\sim 1$  kpc and a potential detector has the effective area  $1 \text{ km}^2$ , we get that about 10 particles could interact with such a detector. In this case the counting rate is  $\sim 10^6 \text{ s}^{-1}$ . And the typical flux created at the neutronization stage is  $10^3$  times smaller. The obtained quantity is much smaller than an expected counting rate of high-energy neutrinos from our Galaxy supernova.

The estimates of the neutrino masses given in Eqs. (5.2), (5.4), and (5.6) does not contradict the modern constraints on the neutrino masses (see, e.g., Ref. [28]). Of course, direct detecting such low-energy neutrinos or antineutrinos is beyond any existing experimental possibilities. The total energy radiated of these neutrino is about  $10^{22}$  erg. This is a completely negli-

gible amount of energy compared to other scales in the supernova problem or in relation to the energy scales in the outer layers of the star. Hence, this flux of created  $\nu\bar{\nu}$  pairs cannot affect the evolution of the star and shows its presence by such a way. Since the flux of low-energy  $\nu\bar{\nu}$  pairs from a supernova has not been detected yet, our constraints on neutrino masses should be regarded as a condition for the creation of a nonvanishing flux of neutrino pairs in matter with the time-dependent effective potential.

Note that the  $\nu\bar{\nu}$  pair creation from the vacuum considered in the present work is the result of a unitary evolution. As a consequence, low-energy particles are coherently emitted in a macroscopic region. The flux of low-energy neutrinos predicted in our work will be accompanied by the radiation of high-energy neutrinos. However, the spectra of highly energetic  $\nu_{e,\mu,\tau}$  and  $\bar{\nu}_{e,\mu,\tau}$  emitted at the neutronization stage of PNS are pinched at low and high-energy parts relative to the mean energy  $\sim 10$  MeV (see details in Appendix A). That is, the very rare  $\nu$  and  $\bar{\nu}$  of such origin can lose enough part of their energy during neutronization to get the considered low-energy range and these particles, produced independently in the reaction between several particles, are statistically independent. It means that, in principle, particles emitted coherently are statistically distinguishable from the latter. The length scale, associated with  $T_\nu$  is  $\sim 10^8$  cm, which is much bigger than both the PNS core radius  $R_c \sim 10$  km and the radius of the sphere where the neutronization happens  $R_n \sim 100$  km. Thus, PNS will be a coherent source of low-energy  $\nu\bar{\nu}$  pairs. These low-energy neutrinos may be involved in some interference effects, e.g., in their lensing by the effective potential barriers of neutron stars and gravity. If we hypothesize that the detection of low-energy neutrinos is possible due to yet unknown mechanism for resonance amplification of the signal, these effects can help one to separate such coherent fluxes from chaotic fluxes of other origin. Currently detecting such low-energy  $\nu$  and  $\bar{\nu}$  seems to be impossible despite the recent theoretical proposals of corresponding experiments of the meV energy scale, see, for example Ref. [29, 30].

## VI. SUMMARY

In this summary we briefly list the main new results obtained in the present work and organize them conditionally into the following three blocks:

(i) We have considered the Dirac neutrino interacting with background fermions in the frame of the standard model. We demonstrate that a time-dependent effective potential is quite possible in a protoneutron star (PNS) at the compression stage just before the hydrodynamic bounce and during PNS neutronization. Such an interaction is intense and must be treated nonperturbatively.

For the first time, we have formulated in the framework of the quantum field theory a corresponding non-

perturbative treatment of neutrino processes in a matter with arbitrary time-dependent effective potential. This allowed us to study analytically a realistic case of slowly varying effective potential. Using complete sets of exact solutions of the Dirac equation in the time-dependent effective potential, we have constructed the initial and final Fock spaces and Bogolyubov transformations between the corresponding creation and annihilation operators. We have expressed mean numbers of  $\nu\bar{\nu}$  pairs created from the vacuum and the probabilities of all the transition processes via coefficients in the Bogolyubov transformations.

(ii) A model with linearly and slowly growing effective potential that has a large difference of its initial and final values compared with the neutrino mass was studied in detail. It was shown that results obtained for this model are representative for a large class of slowly varying potentials. We have calculated differential mean numbers of  $\nu\bar{\nu}$  pair created from the vacuum and have found that they crucially depend on the effective mass of a lightest neutrino. These distributions uniformly span from  $\sim 10^{-6}$  eV to  $\sim 10$  eV energies for  $\nu_{\mu,\tau}\bar{\nu}_{\mu,\tau}$  created due to the compression and from  $\sim 10^{-6}$  eV to  $\sim 0.1$  eV energies for all three active neutrino flavors created due to the neutronization dropping sharply beyond this interval. We have obtained the total number and the energy density of created  $\nu\bar{\nu}$  pairs and examined peculiarities in the production of different neutrino flavors and helicities.

(iii) We have studied  $\nu\bar{\nu}$  pair production from vacuum in a PNS core at the compression stage just before the hydrodynamic bounce and during the PNS neutronization. It was shown that the creation of pairs of low-energy neutrinos up to  $\sim 10$  eV is possible in these cases. These low-energy pairs are coherently emitted from a macroscopic region during the considered stages of the PNS evolution. Part of these particles, depending on the flavor and helicity, are bounded in the PNS while the antineutrinos of any flavor escape the PNS. If the created pairs are  $\nu_e\bar{\nu}_e$  then part of these neutrinos also escape the PNS. Only a part of these escaped neutrinos interacts directly with the uniform matter of electrons and baryons. In general, an effective potential barrier of a neutron star can affect such low-energy neutrinos and antineutrinos, causing refraction and reflection, and, in particular, change their helicity in course of a reflection. Thus, accounting for the characteristic isotropic uniform distribution of  $\nu\bar{\nu}$  pairs created in the low-energy range and specific properties dependent on the neutrino flavors, we have shown that one can distinguish such coherent flux from chaotic fluxes of any other origin. We have derived constraints on the neutrino masses:  $m_{\nu_{\mu,\tau}} \lesssim 4.1 \times 10^{-7}$  eV, for particles created in the core compression before the bounce, as well as  $m_{\nu_e} \lesssim 5.6 \times 10^{-8}$  eV and  $m_{\nu_{\mu,\tau}} \lesssim 1.9 \times 10^{-8}$  eV for the pairs emission at the neutronization, corresponding to the nonvanishing  $\nu\bar{\nu}$  pairs flux produced by this mechanism. We have examined other processes which might affect detection of this vacuum instability in the PNS and found that they are negligible if the mass of the

neutrino is small enough. The energies of created neutrinos are less than 10 eV, for particles emitted before the bounce, and less than 0.1 eV, for the emission at the PNS neutronization. We should mention that  $\bar{\nu}_{\mu,\tau}$  of the pairs created before the bounce freely escape the dense core unlike their high-energy counterparts. Thus these particles can be regarded as precursors of the neutronization neutrino burst. Unfortunately, current experimental techniques do not allow one to detect neutrinos with such low energies.

## ACKNOWLEDGMENTS

M.D. is indebted to FAPESP (Brazil) for a grant and to Y. Kivshar for the hospitality at the ANU where a part of the work was made. S.P. Gavrilov thanks FAPESP for a support and University of São Paulo for the hospitality. D. Gitman thanks CNPq and FAPESP for permanent support.

## Appendix A: ACCOMPANYING PROCESSES

In this Appendix we consider possible processes which might affect either the creation of the neutrino pairs or their subsequent propagation at the initial stages of the PNS evolution. The creation of  $\nu_{\mu,\tau}\bar{\nu}_{\mu,\tau}$  pairs due to the matter compression and their propagation occur before the neutronization. Thus the accompanying processes which can influence these two phenomena do not overlap.

Concerning  $\nu\bar{\nu}$  pairs created at the neutronization, we can conclude the following. We obtain from Eq. (3.26) that a filled neutrino and/or antineutrino initial state blocks the neutrino creation with the corresponding quantum number. However, we see no reason to expect that the occupation numbers of the initial distribution  $N_n^{(\zeta)}$  (in) in the range of low energies being uniformly great immediately after the start of a neutronization stage. As found in Ref. [31], the spectra of highly energetic  $\nu_{e,\mu,\tau}$  and corresponding antiparticles emitted at the neutronization stage of PNS are not Fermi-Dirac ones. In particular these spectra are pinched at low- and high-energy parts relative to the mean energy  $\sim 10$  MeV. For  $\nu_e$  and  $\bar{\nu}_e$  the relaxation time to reach the thermal distribution is longer than  $T_\nu$  [26, 31]. It was revealed in Ref. [32] that for other neutrino species the relaxation time also exceeds  $T_\nu$ . Therefore we get that the creation of low-energy  $\nu\bar{\nu}$  pairs by our mechanism cannot be suppressed by the Pauli factor since the lowest energy states are unoccupied.

It should be noted that besides the  $\nu\bar{\nu}$  pair creation by the spatially homogeneous effective potential  $g(t)$  at the neutronization stage, we can expect that the inhomogeneity of the PNS matter will affect the propagation of low-energy neutrinos escaping the PNS. Let us examine this effect.

For the case of the matter compression, we may roughly assume that the core of PNS has an approximately constant density with  $n_n \sim 10^{38} \text{ cm}^{-3}$ . The PNS core density decreases several orders of magnitude in the spherical PNS crust which has the thickness  $\Delta R_c \sim 1 \text{ km}$  [33]. Taking into account the range of neutrino momenta under consideration given in Eq. (4.37), we see that all low-energy neutrinos and antineutrinos are ultrarelativistic particles. It takes  $\sim 10^{-6} \text{ s}$  for such particles to pass through the PNS crust. The PNS density of the spherical shell of the neutronization,  $10 \text{ km} \lesssim r \lesssim 100 \text{ km}$ , is of the order of  $n_n \sim 10^{36} \text{ cm}^{-3}$ . One can assume that the density of this shell decreases significantly at a distance of  $\sim 10 \text{ km}$  near the outer boundary,  $\Delta R_n \sim 10 \text{ km}$ . The neutrino and antineutrino created due to neutronization are ultrarelativistic particles as well. It takes  $\sim 10^{-5} \text{ s}$  for such particles to escape through the  $10 \text{ km}$  thickness of the outer shell of significant gradient. Both time scales are much shorter than  $T_\nu$ . Therefore we can consider process of the inhomogeneity region crossing as independent one.

To analyze this process we can assume that the effective matter density  $g_{\text{int}} = g(r)$  in the shells of significant gradient varies adiabatically from  $g(t_{\text{in}})$  to  $g(t_{\text{out}})$  and the corresponding gradient of the effective matter density varies smoothly. It is worth mentioning that the size of the wave packet of the low-energy neutrinos under consideration is in the range  $\sim (10^{-5} - 10^2) \text{ cm}$ , which is much smaller than the scale of the matter inhomogeneity.

One can accordingly describe the macroscopic part of these shells using the time-independent one dimensional effective matter density  $g(r)$  that depends only on a radial coordinate  $r$  orthogonal to the border and represents a kind of potential step. We assume that the density  $g(r)$  varies smoothly from the value  $g_{\text{int}}$  in the core to  $g_{\text{ext}} = 0$  in the space outside the shell under consideration with a constant gradient  $a' = -g_{\text{int}}/\Delta R$ .

Thus one can treat the effect of the border using the Dirac equation (2.6) with the matter density  $g(X) = g(r)$ . Such an equation is quite similar to the Dirac equation for the electron in an electric field given by scalar step potential, where  $g(r)/2$  and  $a'/2$  play roles of these potential and constant electric field, respectively. The gradient  $|a'|$  is considerably larger than above mentioned  $|a| \sim (m_{\nu_{e,\mu,\tau}}^{(\text{cr})})^2$  during the compression stage,  $|a'| \sim 10^4 |a|$ , and during the neutronization,  $|a'| \sim 10^2 |a|$ . Hence such a field is very strong for the both subcritical masses given by Eq. (5.2),  $(m_{\nu_{\mu,\tau}}^{(\text{cr})})^2 \ll |a'|$ , and Eqs. (5.4) and (5.6),  $(m_{\nu_{e,\mu,\tau}}^{(\text{cr})})^2 \ll |a'|$ , respectively.

The similar problem of the  $\nu\bar{\nu}$  pairs creation from vacuum in cold neutron stars was considered in Refs. [9, 10] and the production rate of  $\nu\bar{\nu}$  pairs is evaluated following an analogy with Schwinger's result for  $e^+e^-$  creation by a constant uniform electric field [5]. This approach is not applicable for our problem since it does not allows us to

estimate the mean number of particles created within a finite time  $T$  on a finite length  $\Delta R$ . In our case a more detailed analysis is required, analogous to that made in Refs. [34–36] where the  $e^+e^-$  pair creation by a constant uniform electric field given by scalar potential was studied.

The differential mean number of neutrino or antineutrino created from vacuum by the inhomogeneous matter can be evaluated in analogy with the case of the electric field, yielding

$$N_n^{\text{gr}} \approx \exp \left[ -2\pi (m^2 + \mathbf{p}_\perp^2) / |a'| \right], \quad (\text{A1})$$

where  $m$  is the corresponding neutrino mass,  $n = (p_0, \mathbf{p}_\perp, s)$  is the complete set of quantum numbers,  $p_0$  is the total energy,  $\mathbf{p}_\perp$  is transversal momentum that is orthogonal to the gradient direction, and  $s$  is a given spin polarization. Note that the distribution  $N_n^{\text{gr}}$  decreases very rapidly with increasing transversal momentum.

It can be shown that the expression given by Eq. (A1) is valid in the range of the energy  $|p_0| < |g_{\text{int}}|/2$  and the value of  $N_n^{\text{gr}}$  is negligible outside this range. The accurate nonperturbative treatment of  $\nu\bar{\nu}$  pairs creation due to the inhomogeneity of the matter density can be performed using the formalism recently developed in Ref. [8]. The appropriate general QFT formalism is developed in Ref. [37]. Note that the value given by Eq. (A1) saturates for low values of  $\mathbf{p}_\perp^2$ ,  $N_n^{\text{gr}} \simeq 1$  for the subcritical masses,  $m \lesssim m_{\nu_{e,\mu,\tau}}^{(\text{cr})}$ . The total number of particles created by this mechanism can be found as

$$\mathcal{N}^{\text{gr}} \approx \frac{T_\nu S_R}{(2\pi)^3} \sum_{s=\pm 1} \int N_n^{\text{gr}} dp_0 d\mathbf{p}_\perp, \quad (\text{A2})$$

where  $S_R$  is the area of the corresponding outer surface of the PNS shell of significant gradient.

To get an estimate we write down that

$$\mathcal{N}^{\text{gr}} \approx \frac{T_\nu S_R |g_{\text{int}}| |a'|}{2(2\pi)^3}. \quad (\text{A3})$$

The ratio of this value and the total numbers  $\mathcal{N}_\sigma$  given by Eqs. (4.27), (4.32), (4.35), and (4.38) is

$$\begin{aligned} \mathcal{N}^{\text{gr}}/\mathcal{N}_\sigma &\sim e^{\pi\lambda} T_\nu (R\Delta R |g_{\text{int}}|)^{-1} \\ &\sim \begin{cases} 10^{-7} e^{\pi\lambda} & \text{for compression} \\ 10^{-6} e^{\pi\lambda} & \text{for neutronization} \end{cases}, \quad (\text{A4}) \end{aligned}$$

where we use that  $R\Delta R = R_c\Delta R_c = 10 \text{ km}^2$  for the compression and  $R\Delta R = R_n\Delta R_n = 10^3 \text{ km}^2$  for the neutronization. Thus, despite the fact that the vacuum instability effects caused by the PNS shells of density gradient are very pronounced for the neutrinos with the subcritical masses (in this case  $\lambda \lesssim 1$ ), they are negligible during the initial stages of the PNS evolution and cannot block the  $\nu\bar{\nu}$  pair creation due to the time-dependent effective potential. We note, however, that the ratio in Eq. (A4) is very sensitive to the neutrino mass. If the mass of the lightest neutrino is sufficiently greater than

the critical values given by Eqs. (5.2), (5.4), and (5.6),  $\lambda \gg 1$ , so that the ratio (A4) is not small,  $\mathcal{N}^{crust}/\mathcal{N}_\sigma \gtrsim 1$ , then the effects caused by the density gradients must be taken into account. Thus, our mechanism of the  $\nu\bar{\nu}$  pair creation is valid if  $\lambda \lesssim 1$ .

The nonzero difference between the effective density  $g_{\text{int}}$  in the region of creation and  $g_{\text{ext}} \approx 0$  in the space outside this region affects the results of the  $\nu\bar{\nu}$  pair creation due to the time-dependent effective potential for a distant observer. To see that we consider the radial motion of neutrinos and antineutrinos through the PNS shells of density gradient, assuming that  $\mathbf{p}_\perp \approx 0$ . Using the Dirac equation (2.6) with the matter density  $g(r)$ , we see that, in general, the helicity is not conserved when a neutrino moves in the inhomogeneous matter. However, if  $\mathbf{p}_\perp \approx 0$  the projection of the spin on the radial direction is conserved. Note that this projection is not related to the direction of the momentum vector then the helicity is not necessary conserved anyway. The total energy of particles and antiparticles  $p_0^{(\pm)}$  is conserved. Using Eq. (2.6), one can elaborate the following asymptotic dispersion relations for a given value of  $p_0^{(\pm)}$ :

$$\begin{aligned} p_0^{(\pm)} &= \frac{g_{\text{int}}}{2} \pm \mathcal{E}_{\text{int}}, \quad \mathcal{E}_{\text{int}} = \sqrt{m^2 + p_{\text{int}}^2} \\ &\quad \text{in the region of creation;} \\ p_0^{(\pm)} &= \pm \mathcal{E}_{\text{ext}}, \quad \mathcal{E}_{\text{ext}} = \sqrt{m^2 + p_{\text{ext}}^2} \\ &\quad \text{outside the region of creation.} \end{aligned} \quad (\text{A5})$$

Here  $\mathcal{E}_{\text{int}}$ ,  $\mathcal{E}_{\text{ext}}$  are the corresponding asymptotic values of the particle kinetic energy and  $p_{\text{int}}$ ,  $p_{\text{ext}}$  are the magnitudes of the corresponding radial momenta  $p_{\text{int}} = |\mathbf{p}_{\text{int}}|$ ,  $p_{\text{ext}} = |\mathbf{p}_{\text{ext}}|$ , respectively.

Assuming that  $g_{\text{int}} = g(t)$  in the region of creation varies adiabatically from  $g(t_{\text{in}})$  to  $g(t_{\text{out}})$ , we consider the case when  $\mathcal{E}_{\text{int}}$  is the energy of neutrino or antineutrino with a given  $\sigma$  created from vacuum by the neutronization until the time  $t$ ,  $\mathcal{E}_{\text{int}} = \mathcal{E}_2$ , where  $\mathcal{E}_2$  is given by Eq. (3.14) at  $g_2 = g_{\text{int}}$ . Then  $p_{\text{int}} = |p - \sigma g_{\text{int}}/2|$  and the ranges of momentum are given by Eqs. (4.31) and (4.34) at  $g_2 = g_{\text{int}}$ . Taking into account the fact that the main fraction of the  $\nu\bar{\nu}$ -pairs with  $\sigma = -1$  for all flavors are created due to the neutronization at the time  $t$  when

$$\begin{aligned} g_{\text{int}} < 0; \quad |g_{\text{int}}| > \sqrt{2aK} \quad \text{for } \nu_e \bar{\nu}_e, \\ |g_{\text{int}}| > |g(t_{\text{in}})| + \sqrt{2aK} \quad \text{for } \nu_{\mu,\tau} \bar{\nu}_{\mu,\tau}, \end{aligned}$$

we find from Eq. (A5) that all of these neutrinos are bounded in the PNS while all of these antineutrinos gain additional kinetic energy  $\sim |g_{\text{int}}|/2$  and escape the PNS with the energy  $\mathcal{E}_{\text{ext}} \approx |g_{\text{int}}| - p$ . It is consistent with the general conclusion obtained earlier for neutron stars in Refs. [9–11]. For all  $\nu_{\mu,\tau} \bar{\nu}_{\mu,\tau}$  pairs created due the compression we have  $\sigma = -1$  and  $g_{\text{int}} < 0$ . Note that the projection of the kinetic momentum on the direction of the momentum of this antineutrino,  $p - |g_{\text{int}}| < 0$ , then its physical helicity outside the region of creation is negative. Such kind of antineutrino does not substantially

interact with the matter of electrons and baryons, unless it interacts with a potential barrier, then it is considered undetectable. The final effective density  $g_{\text{int}} = g(t_{\text{out}})$  retains its value during the entire period of the existence of a neutron star then these neutrinos are the trapped forever. Thus, we estimate the time-depending range of the antineutrino kinetic energy outside the PNS during the neutronization as follows

$$\begin{aligned} \frac{|g_{\text{int}}|}{2} < \mathcal{E} < |g_{\text{int}}| \quad \text{for } \bar{\nu}_e, \\ \frac{1}{2} (|g(t_{\text{in}})| + |g_{\text{int}}|) < \mathcal{E} < |g_{\text{int}}| \quad \text{for } \bar{\nu}_{\mu,\tau}. \end{aligned} \quad (\text{A6})$$

The range of the  $\bar{\nu}_{\mu,\tau}$  kinetic energy outside the PNS during the compression is

$$\frac{|g_{\text{int}}|}{2} < \mathcal{E} < |g_{\text{int}}|. \quad (\text{A7})$$

When the neutronization stage ended, the spherical layer of ultrarelativistic antineutrinos with the kinetic energies in the range

$$\begin{aligned} \sqrt{a/2K} < \mathcal{E} < |g(t_{\text{out}})| \quad \text{for } \bar{\nu}_e, \\ |g(t_{\text{in}})| + \sqrt{a/2K} < \mathcal{E} < |g(t_{\text{out}})| \quad \text{for } \bar{\nu}_{\mu,\tau} \end{aligned} \quad (\text{A8})$$

is formed outside the PNS and then expands at a speed close to the speed of light. When the compression stage ended, the spherical layer of  $\bar{\nu}_{\mu,\tau}$  with the kinetic energies in the range

$$\sqrt{a/2K} < \mathcal{E} < |g(t_{\text{out}})| \quad (\text{A9})$$

is formed outside the PNS and then expands.

We point out first that for the part of the  $\nu_e \bar{\nu}_e$  pairs created with the helicity quantum number  $\sigma = +1$  due to the neutronization, the effect of the PNS border is completely different. It was shown in Eq. (4.31) that such particles are created before the effective density  $g(t) > 0$  passes through zero at some time  $t_0$  and have the maximal kinetic energy per particle  $\sim \frac{1}{2}g(t_{\text{in}})$  at  $t_0$ . Therefore, the positive value  $g_{\text{int}} = g(t)$  varies from  $g(t_{\text{in}})$  to zero, meanwhile the maximal kinetic energy of created  $\nu_e$  or  $\bar{\nu}_e$  increases from zero to  $\frac{1}{2}g(t_{\text{in}})$ . If  $p > g_{\text{int}}/2$ , then both  $\nu_e$  and  $\bar{\nu}_e$  escape the PNS and the time-depending range of the kinetic energy outside the PNS during the neutronization is

$$\begin{aligned} \sqrt{a/2K} < \mathcal{E} < g(t_{\text{in}})/2 \quad \text{for } \nu_e, \\ 0 < \mathcal{E} < g(t_{\text{in}})/2 - g_{\text{int}} \quad \text{for } \bar{\nu}_e. \end{aligned} \quad (\text{A10})$$

Their helicity quantum number outside the crust is conserved. Such a fraction of the  $\nu_e \bar{\nu}_e$  is considered undetectable directly.

If  $p < g_{\text{int}}/2$  and  $g_{\text{int}} > \sqrt{a/2K}$ , then these  $\bar{\nu}_e$  are bounded in the PNS until the time when  $g_{\text{int}}$  will be small enough and then escape with helicity conserved. All of these  $\nu_e$  gain additional kinetic energy  $\sim g_{\text{int}}/2$  and escape the PNS with the energy  $\mathcal{E}_{\text{ext}} \approx g_{\text{int}} - p$ . The



projection of the kinetic momentum on the direction of the momentum of this  $\nu_e$ ,  $p - g_{\text{int}} < 0$ , then its physical helicity outside the PNS is negative. Such neutrinos interact with the matter of electrons and baryons and are detectable in principle. We estimate the time-depending range of the neutrino kinetic energy outside the region of creation during the neutronization as

$$g_{\text{int}}/2 < \mathcal{E} < g_{\text{int}} - \sqrt{a/2}K. \quad (\text{A11})$$

This range shrinks to the point when time  $t$  tend to  $t_0$ . As a result, when the neutronization stage ended, the spherical layer of such ultrarelativistic neutrinos with the kinetic energies in the range

$$0 < \mathcal{E} < g(t_{\text{in}}) - \sqrt{a/2}K \quad (\text{A12})$$

is formed outside the PNS and then expands at a speed close to the speed of light.

Thus, only electron neutrinos of all  $\nu\bar{\nu}$  pairs created during the neutronization stage can be in principle detected directly by a distant observer. However, note that the effective potential of a neutron star is repulsive for the low-energy antineutrinos escaped the PNS. Then these antineutrinos can change their helicity if reflected of a neutron star. In general, the effective potential of a neutron star can considerably refracts such low-energy  $\nu$  and  $\bar{\nu}$ .

From the beginning we have neglected the influence of gravity and rotation. However, PNS can have rather strong gravitational field and rotate rapidly. In principle these effects can influence the creation of  $\nu\bar{\nu}$  pairs and their subsequent evolution especially since energies of particles are small. For example, as was found in Ref. [38], very low-energy antineutrinos can be captured inside a rotating PNS. The characteristic length scale associated with gravity or rotation of PNS is in the km range. Indeed, it can be a gravitational radius which is several km for a PNS with the mass in the solar range. The energy corresponding to such a length scale is  $\sim (10^{-10} - 10^{-9})$  eV. In our situations the typical energies of  $\nu\bar{\nu}$  pairs are up to several eV or up to 0.1 eV. Thus gravity and rotation can affect only very narrow part near the bottom of the spectrum of  $\nu\bar{\nu}$  pairs created. Nevertheless gravity can influence the propagation of created neutrino beam while it propagates further in space. By the same reason a cosmic neutrino background, expected at 1.95 K  $\sim 0.17$  meV, is irrelevant for the case under consideration.

The coherent  $\nu\bar{\nu}$  pairs creation discussed in our work is not influenced by the pairs creation by nucleon-nucleon bremsstrahlung. Indeed, using the results of Ref. [39] one gets that  $\nu\bar{\nu}$  pairs created in nucleon-nucleon bremsstrahlung have energy  $\sim 1$  MeV in nuclear matter with temperature  $T \sim 10^9$  K, which is typical for a core collapsing supernova. Thus this process does not overlap with the pairs creation by our mechanism.

## Appendix B: SOME PROPERTIES OF WEBER PARABOLIC CYLINDER FUNCTIONS

In this appendix we list some properties of the WPCFs which are used in the present work and where already

used by us studying particle creation from the vacuum by a quasiconstant uniform electric field, see Ref. [22].

The solution of the ordinary differential equation

$$\left[ \frac{d^2}{dz^2} + \rho + \frac{1}{2} - \frac{z^2}{4} \right] \varphi(z) = 0, \quad (\text{B1})$$

can be expressed as a linear combination of any of two functions from the following set:  $D_\rho(z)$ ,  $D_\rho(-z)$ ,  $D_{-\rho-1}(iz)$ , and  $D_{-\rho-1}(-iz)$ . If we change the variable  $z = (1-i)\xi$  in Eq. (4.10), we can represent it in the form of Eq. (B1) with  $\rho = i\lambda/2 + [\chi \text{sgn}(a) - 1]/2$ . Then assuming that  $\chi \text{sgn}(a) = +1$ , we obtain linear independent solutions of Eq. (4.10) used in Sec. IV. Note that a more detailed description of the properties of the WPCFs can be found, e.g., in Ref. [40].

The asymptotic expansions of WPCF, used in Sec. IV, corresponding to the great absolute values of the argument  $|\xi|$ , have the following form:

$$\begin{aligned} D_\rho[(1 \pm i)\xi] &= e^{\mp i\xi^2/2} \left( \sqrt{2}e^{\pm i\pi/4}\xi \right)^\rho \\ &\times \left[ 1 \mp i \frac{\rho(1-\rho)}{4\xi^2} + \dots \right] \\ &\text{if } \xi \geq K, \end{aligned} \quad (\text{B2})$$

where  $K \gg \max\{1, \lambda\}$ . If  $\xi < 0$  one gets that

$$\begin{aligned} D_\rho[(1-i)\xi] &= e^{i\pi\rho} D_\rho[(1-i)|\xi|] + i \frac{\sqrt{2\pi}}{\Gamma(-\rho)} e^{i\pi\rho/2} \\ &\times D_{-\rho-1}[(1+i)|\xi|], \\ D_{-\rho-1}[(1+i)\xi] &= e^{i\pi(\rho+1)} D_{-\rho-1}[(1+i)|\xi|] \\ &- i \frac{\sqrt{2\pi}}{\Gamma(\rho+1)} e^{i\pi(\rho+1)/2} \\ &\times D_\rho[(1-i)|\xi|], \end{aligned} \quad (\text{B3})$$

where  $\Gamma(z)$  is the Euler gamma function.

Using Eqs. (B2) and (B3), we get the expansions of the coefficients  $f_k(t_l)$ ,  $k, l = 1, 2$ , which are required for the calculation of the expression  $B$  given by Eq. (4.16),

$$\begin{aligned} f_1(t) &\approx O(\xi^{-3}), \\ f_2(t) &\approx e^{i\xi^2/2} \left( \sqrt{2}e^{-i\pi/4}\xi \right)^\rho [2 + O(\xi^{-2})] \\ &\text{if } \xi \geq K; \\ f_1(t) &\approx e^{i\pi(\rho+1)} e^{-i\xi^2/2} \left( \sqrt{2}e^{i\pi/4}|\xi| \right)^{-\rho-1} \\ &\times [2 + O(|\xi|^{-2})], \\ f_2(t) &\approx O(|\xi|^{-1}) \quad \text{if } \xi < 0, |\xi| \geq K. \end{aligned} \quad (\text{B4})$$

- 
- [1] W. Greiner, B. Müller and J. Rafelsky, *Quantum Electrodynamics of Strong Fields* (Springer-Verlag, Berlin, 1985).
- [2] N. D. Birrell and P. C. W. Davies, *Quantum Fields in Curved Space* (Cambridge University Press, Cambridge, 1982); A. A. Grib, S. G. Mamaev, and V. M. Mostepanenko, *Vacuum Quantum Effects in Strong Fields* (Friedmann Laboratory Publishing, St. Petersburg, 1994); R. Ruffini, G. Vereshchagin and S. Xue, Phys. Rep. **487**, 1 (2010).
- [3] D. M. Gitman, J. Phys. A **10**, 2007(1977); E. S. Fradkin, and D. M. Gitman, Fortschr. Phys. **29**, 381 (1981); E. S. Fradkin, D. M. Gitman, and S. M. Shvartsman, *Quantum Electrodynamics with Unstable Vacuum* (Springer-Verlag, Berlin 1991)
- [4] S. P. Gavrilov, D. M. Gitman, and J. L. Tomazelli, Nucl. Phys. B **795**, 645 (2008); hep-th/0612064.
- [5] J. Schwinger, Phys. Rev. **82**, 664 (1951).
- [6] G. V. Dunne, Eur. Phys. J. D **55**, 327 (2009).
- [7] S. P. Gavrilov, D. M. Gitman, and N. Yokomizo, Phys. Rev. D **86**, 125022 (2012); arXiv:1207.1749.
- [8] S. P. Gavrilov and D. M. Gitman, Phys. Rev. D **87**, 125025 (2013); arXiv:1211.6776.
- [9] A. Loeb, Phys. Rev. Lett. **64**, 115 (1990); Erratum *ibid.* **64**, 3203 (1990).
- [10] M. Kachelrieß, Phys. Lett. B **426**, 89 (1998); hep-ph/9712363.
- [11] K. Kiers and N. Weiss, Phys. Rev. D **56**, 5776 (1997).
- [12] A. Kusenko and M. Postma, Phys. Lett. B **545**, 238 (2002); hep-ph/0107253.
- [13] H. Koers, Phys. Lett. B **605**, 384 (2005); hep-ph/0409259.
- [14] F. An, *et al.*, (Daya Bay Collaboration) Phys. Rev. Lett. **108**, 171803 (2012); arXiv:1203.1669 [hep-ex]; Y. Abe, *et al.*, (Double Chooz Collaboration), Phys. Rev. Lett. **108**, 131801 (2012); arXiv:1112.6353 [hep-ex]; J. K. Ahn, *et al.*, (RENO Collaboration), Phys. Rev. Lett. **108**, 191802 (2012); arXiv:1204.0626 [hep-ex].
- [15] M. Agostini, *et al.*, (GERDA Collaboration), Phys. Rev. Lett. **111**, 122503 (2013); arXiv:1307.4720 [nucl-ex]; M. Auger, *et al.*, (EXO Collaboration), Phys. Rev. Lett. **109**, 032505 (2012); arXiv:1205.5608 [hep-ex].
- [16] H. Nunokawa, V. B. Semikoz, A. Yu. Smirnov, and J. W. F. Valle, Nucl. Phys. B **501**, 17 (1997); hep-ph/9701420.
- [17] M. Dvornikov and A. Studenikin, J. High Energy Phys. **09** (2002) 016; hep-ph/0202113.
- [18] W. Keil, H.-Th. Janka, and E. Müller, Astrophys. J. Lett. **473**, L111 (1996); astro-ph/9610203.
- [19] M. Dvornikov and D. M. Gitman, Phys. Rev. D **87**, 025027 (2013); arXiv:1211.5367 [hep-th].
- [20] A. Studenikin and A. Ternov, Phys. Lett. B **608**, 107 (2005); hep-ph/0412408.
- [21] V. B. Berestetskii, E. M. Lifschitz, and L. P. Pitaevskii, *Quantum Electrodynamics* (Pergamon, Oxford, 1989), 2nd ed., p. 86.
- [22] S. P. Gavrilov and D. M. Gitman, Phys. Rev. D **53**, 7162 (1996); hep-th/9603152.
- [23] R. N. Cahn, *et al.*, *White Paper: Measuring the Neutrino Mass Hierarchy*; arXiv:1307.5487 [hep-ex].
- [24] A. Heger, C. Fryer, S. Woosley, N. Langer, and D. Hartmann, Astrophys. J. **591**, 288 (2003); astro-ph/0212469.
- [25] H.-Th. Janka, K. Langanke, A. Mareka, G. Martínez-Pinedo, and B. Müller, Phys. Rept. **442**, 38 (2007); astro-ph/0612072.
- [26] T. A. Thompson, A. Burrows, and P. A. Pinto, Astrophys. J. **592**, 434 (2003); astro-ph/0211194.
- [27] C. Giunti and C. W. Kim, *Fundamentals of Neutrino Physics and Astrophysics* (Oxford University Press, Oxford, 2007), pp. 160–179.
- [28] V. N. Aseev, *et al.*, Phys. Rev. D **84**, 112003 (2011); arXiv:1108.5034 [hep-ex]; K. N. Abazajian, *et al.*, Astropart. Phys. **35**, 177 (2011); arXiv:1103.5083 [astro-ph.CO]; A. D. Dolgov, K. Kainulainen, and I. Z. Rothstein, Phys. Rev. D **51**, 4129 (1995); hep-ph/9407395.
- [29] M. Yoshimura, Phys. Rev. D **75**, 113007 (2007); T. Takahashi and M. Yoshimura, *Effect of Relic Neutrino on Neutrino Pair Emission from Metastable Atoms*, arXiv:hep-ph/0703019; A. Fukumi *et al.*, Progr. Theor. Exp. Phys. **2012**, 04D002 (2012) [arXiv:1211.4904]; M. Yoshimura, N. Sasao, *Radiative emission of neutrino pair from nucleus and inner core electrons in heavy atoms*, arXiv:1310.6472.
- [30] A. Cocco, G. Magnano, and M. Messina, JCAP **0706**, 015 (2007); J. Phys. Conf. Ser. **110** (2008) 082014; A. Faessler, R. Hodak, S. Kovalenko, and F. Simkovic, *Search for the Cosmic Neutrino Background and KATRIN*, arXiv: 1304.5632; J.D. Vergados, Yu. N. Novikov, *Prospects of detection of relic antineutrinos by resonant absorption in electron capturing nuclei*, arXiv:1312.0879.
- [31] T. Totani, K. Sato, H. E. Dalhed, and J. R. Wilson, Astrophys. J. **496**, 216 (1998), astro-ph/9710203.
- [32] T. A. Thompson, A. Burrows, and J. E. Horvath, Phys. Rev. C **62**, 035802 (2000); astro-ph/0003054.
- [33] P. Haensel, A. Y. Potekhin, and D. G. Yakovlev, *Neutron Stars I: Equation of State and Structure*, (Springer, New York, 2007), pp. 11–14.
- [34] A. I. Nikishov, Nucl. Phys. **B21**, 346 (1970).
- [35] A. I. Nikishov, *Quantum Electrodynamics of Phenomena in Intense Fields* Proceedings of P.N. Lebedev Physics Institute Vol. **111** (Nauka, Moscow, 1979), p. 153.
- [36] R. C. Wang and C. Y. Wong, Phys. Rev. D **38**, 348 (1988).
- [37] S. P. Gavrilov and D.M. Gitman, *QFT formulation of particle creation by potential steps*, unpublished.
- [38] A. I. Studenikin, J. Phys. A **41**, 164047 (2008); arXiv:0804.1417 [hep-ph].
- [39] G. G. Raffelt, *Stars as Laboratories for Fundamental Physics* (University of Chicago Press, Chicago, 1996), p. 130
- [40] *Higher Transcendental functions* (Bateman Manuscript Project), edited by A. Erdelyi *et al.*, Vol.2 (McGraw-Hill, New York, 1953).